FAR-INFRARED ABSORPTION BY EXCITONS IN GERMANIUM AT HIGH CONCENTRATIONS

By

© STELLA NINA KRAUZEWICZ, B.Sc.

A Thesis

Submitted to the School of Graduate Studies

in Partial Fulfilment of the Requirements

for the Degree

Master of Science

McMaster University

December 1981

FAR-INFRARED ABSORPTION BY EXCITONS IN GERMANIUM AT HIGH CONCENTRATIONS

MASTER OF SCIENCE (1981) McMASTER UNIVERSITY
(Physics) Hamilton, Ontario

TITLE: Far-infrared Absorption by Excitons in Germanium at High Concentrations

AUTHOR: Stella Nina Krauzewicz, B.Sc. (University of Sussex, England)

SUPERVISOR: Dr. T. Timusk

NUMBER OF PAGES: vii, 70

ABSTRACT

The dependence on frequency of the photo-ionization cross-section of indirect excitons in germanium (at concentrations corresponding to "isolated" excitons) was found to be $\nu^{-1.5}$. A dependence of $\nu^{-2.7}$ had been expected, by comparison with the hydrogen theory previously thought applicable. No adequate replacement theory exists. A probable explanation might lie in the Lucovsky model of impurities in semiconductors, which predicts the correct frequency dependence, assuming an enhanced interparticle potential at small separations. This central cell correction was justified in excitons because the dielectric constant of the material varies with the electron-hole separation. The - 1.5 power was found to decrease slowly as concentration increased.

The main observation at concentrations of 2×10^{14} cm^{-3} and above was a new, strongly absorbing, component of non excitonic character in the absorption spectrum between 1 and 2 meV, peaking at 1.5 meV with a FWHM of $\sim$ 1 meV. The peak grew at the 1.5th power of the exciton peaks, having a fairly sharp onset between 4 and 5.5°K and a very small temperature dependence above that range. This peak was interpreted in terms of an electron-hole plasma analogous to ordinary electron-hole fluid, which appeared in the form of drops in the high density

exciton cloud. A double peaked phase diagram was constructed, in qualitative agreement with some theoretical predictions, and experimental results obtained by workers using the recombination luminescence technique, some of whom attribute their results to the formation of biexcitons.

ACKNOWLEDGEMENTS

I would like to thank my supervisor, Dr. T. Timusk, for his advice and help during my work at McMaster.

The laboratory work was eased by the instruction in the use of the equipment by Dr. Graciela Zárate, also Frank Lin, and the help of Carlos Zárate and Andy Duncan who machined and aided in the design of various parts. The other technical support staff must not be forgotten.

I would like to thank Dr. D. Taylor for his support, and help with reviewing some of the thesis sections.

I am grateful to Mrs. Helen Kennelly for typing this thesis with unbelievable speed.

Lastly, I would like to thank my husband, Dr. Martin Elliott, for discussions, support and encouragement throughout this time.

TABLE OF CONTENTS

LIST OF FIGURES

CHAPTER 1

INTRODUCTION

In this work the technique of absorption of far-infrared radiation was used to study two aspects of the behaviour of excitons in germanium: the frequency variation of the ionization cross-section of the excitons, and the nature of the excitonic matter at high concentrations.

Existing experimental systems were used to study the photoionization cross-section at low to medium concentrations, that is, with n_{ex}, the number of excitons, between 10^{12} cm^{-3} and 2×10^{14} cm^{-3}, at temperatures of between four and ten degrees Kelvin. This topic has not been extensively studied: only one reference is available (Buchanan and Timusk 1976). The results of our experiments suggest an inadequacy in the standard exciton theory (the effective mass model), which compares the exciton to the hydrogen atom.

A new system had to be developed in order to study high concentrations of excitons (2×10^{14} cm^{-3} and above), the attainment of which presented much greater experimental difficulties.

The high concentration region is of great interest and controversy. There is a possibility of observing a metal-insulator transition between excitons and a conducting electron-hole

plasma, at approximately $n_{ex} = 1.6\times10^{15}$ cm^{-3}. At around this concentration the exact structure of the phase diagram relating excitons, electron-hole fluid and plasma is unknown. These problems have been studied fairly extensively in the past using the recombination luminescence technique, with different authors giving different interpretations to their results, for example Thomas and Rice (1977); and Balslev and Furneaux (1979). We hoped to gain new insights into the problem by using the far-infrared absorption technique instead. A new component in the absorption spectrum, in a region where at lower concentrations and these temperatures little absorption is seen, was observed.

Chapter two presents an introduction to excitons and the basic theoretical model used to explain their behaviour in spectroscopic experiments. The basic experimental system is also reviewed. Chapter three discusses the photoionization experiments in the lower concentration regime giving experimental details, theory, results and discussion, and chapter four deals with the high concentration regime in a similar way. Chapter five presents a discussion of the work as a whole, and suggestions for future experiments.

CHAPTER 2

INTRODUCTORY THEORY AND EXPERIMENTAL TECHNIQUES

(i) Introduction to Excitons

Semiconductors and insulators are characterized by the fact that there exists a forbidden region in the band structure below which, at absolute zero, the valence band states are all filled and above which, the conduction bands are empty. The smallest energy required to move an electron from a state in the valence band to one in the conduction band is known as the band gap energy, E_g. This gap may be direct or indirect, that is the initial and final states may have the same, or a different reciprocal space wavevector, k. The value of E_g for germanium, the semiconductor used in this work, is 0.74 eV at 0°K and 0.67 eV at 300°K. In germanium the gap is indirect: the maximum of the valence band occurs at the centre of the Brillouin zone and the minimum of the conduction band in the <111> direction at the zone boundary. Because of the symmetry of the crystal (germanium has the diamond structure, a face centred cubic lattice with a basis of two atoms - at 0 and $(\frac{1}{4},\frac{1}{4},\frac{1}{4})$) there are eight of these points on the Brillouin zone. The valence band maximum would be six fold degenerate, were it not for spin orbit coupling, which separates a two-fold "split-off" band, 0.29 eV lo-

Figure 2-1

Schematic energy band structure of germanium (after G. Zárate, 1981).

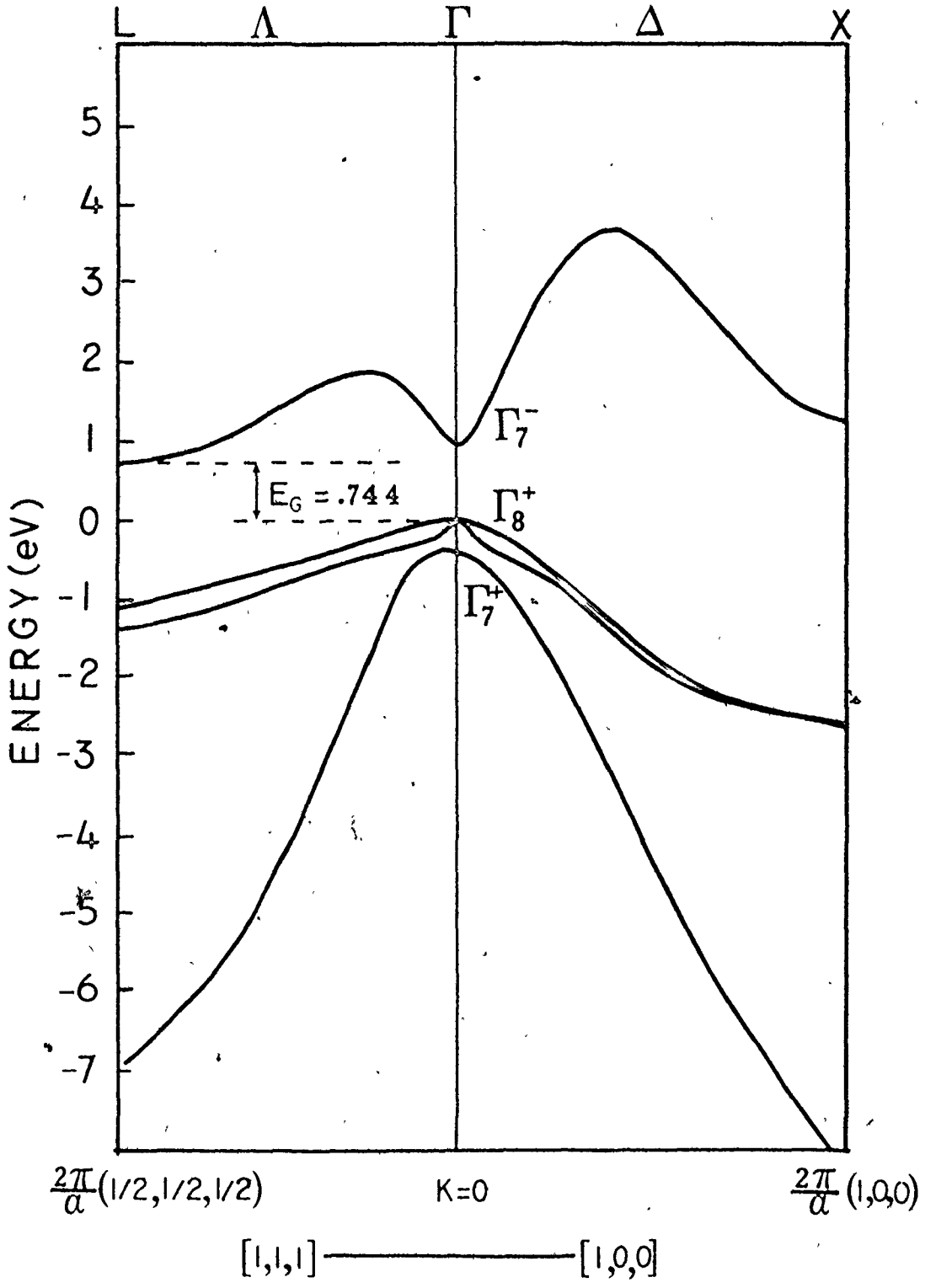
L
Λ
Γ
Δ
X
5
4
3
2
1
0
-1
-2
-3
-4
-5
-6
-7
ENERGY (eV)
E_G = .744
Γ_7^-
Γ_8^+
Γ_7^+
$\frac{2\pi}{a}$(1/2,1/2,1/2)
K=0
$\frac{2\pi}{a}$(1,0,0)
[1,1,1]
[1,0,0]

wer. The remaining fourfold band splits into two twofold bands away from $k \neq 0$, the light and heavy hole bands, so named because of the band effective masses arising from their curvature. The constant energy surfaces arising from the band structure vary in shape from nearly spherical for the light holes and less so for the heavy holes, to extremely elongated ellipsoids for the electrons in the conduction band.

Optical absorption experiments performed in semiconductors and insulators show absorption below the gap energy, however, and the absorption edge shows structure instead of a sharp onset. The explanation for this phenomenon is the formation of excitons.

When an electron is excited into the conduction band, a hole is created in the valence band. Being of opposite charge, they can attract one another and form a bound pair, rather like a hydrogen atom or positronium. The binding energy accounts for the discrepancy between the expected and experimentally observed onset of absorption.

In a direct gap semiconductor this process takes place exactly as described but in an indirect gap material a phonon must be absorbed or emitted in the process, because the wavevector of the final state of the electron is not the same as that of the initial. The excitons are thus referred to as direct or indirect. The reverse process, in which the electron and hole recombine can also occur. Since a three body process (electron, hole and phonon) is more unlikely to occur than a two body one

the indirect excitons are more stable than the direct excitons with respect to decay. The lifetimes of the direct and indirect excitons in germanium are $\sim 10^{-7}$ and $\sim 10^{-5}$ seconds, respectively (Kittel 1976).

Excitons may be mobile within the crystal or fixed, for example bound to an impurity. Excitons in germanium may move as much as one millimetre within their lifetime (Pokrovskii and Svistunova 1971). The movement may be merely the result of diffusion or in response to a strain gradient, for example.

Excitons can be tightly or loosely bound and are then known as Frenkel or Mott/Wannier excitons respectively. The Frenkel exciton is localised on one atom on the solid although it is possible to transfer the excitation from one atom to another, enabling the exciton to move. This type of exciton typically occurs in insulators; the binding energy of the excitons is of the order of electron volts (eV). The Mott or Wannier exciton, by contrast, has a much larger spacing - of the order of twenty atomic spacings for germanium - with a binding energy of the order of milli-electron volts (meV). The two pictures are opposite extremes of a range, excitons may lie anywhere in between.

A recent review of the theory used to describe the theory of the exciton was given by Altarelli and Lipari (1976). This theory is known as the effective mass model, because the electron is regarded as a particle with the electronic charge and a mass

corresponding to the band effective mass of the energy minimum of the conduction band. Similarly the hole is regarded as a particle with a positive electronic charge, and mass corresponding to that of the maximum of the valence band. These interact electrostatically; and the Hamiltonian describing the exciton consists merely of the electron Hamiltonian and the hole Hamiltonian plus a term describing the Coulomb interaction between them, Dresselhaus (1956), modified only by the static dielectric constant of the semiconductor, ε. In this approximation the electron-hole exchange interaction, the wavevector and frequency dependence of ε, and polaron effects are neglected. Germanium is not a polar crystal, and has high ε and low effective mass which lead to large orbits minimising exchange, and therefore fits this model very well.

The various terms in the exciton Hamiltonian can be arranged in groups with different symmetries - spherical, cubic and axial. If, such as in the case for a direct gap semiconductor, there is no axial term, the corrections to a hydrogenic Hamiltonian are small, and can be handled by perturbation theory. In indirect gap semiconductors there is a large axial term due to the anisotropy of the electron mass, which produces major changes in the hydrogen level scheme.

The problem is simplified if the valence band is assumed to be axially symmetric about the long axis of the conduction band ellipsoid - the so called "axial model" for indirect ex-

citons. Values for the ground state and splitting of the ground state of the excitons in germanium, silicon and gallium phosphide, calculated in this way, match experiment very well.

Thus in germanium we have a system which behaves qualitatively as a hydrogen atom, but quantitatively differs substantially: levels which would have been degenerate in hydrogen now have large splittings, and levels are shifted with respect to a hydrogen-like pattern.

As is the case for hydrogen the "gas" atoms can condense into fluid (électron-hole fluid), ionise into a plasma of electrons and holes, form molecules (biexcitons) which can ionise (trions). The trions can consist of one electron and two holes or one hole and two electrons. Higher numbers of excitons can be bound into multi-exciton complexes. It has been suggested that both excitons and excitonic molecules can undergo Bose condensation, although excitons are not strictly bosons, as discussed by Haken (1976).

A very interesting topic is the possibility of a metal-insulator or Mott transition occurring in the atomic gas phase. With increasing density the individual excitons become dissociated so that a conducting plasma rather than an insulating gas is obtained. It is not clear whether this has yet been observed experimentally. This topic will be discussed further in chapter four. The phases of excitonic matter that are easiest to observe are the atomic gas, the liquid phase, and mixtures of the

two. The conditions of temperature and density required are most easily represented in the phase diagram.

As the concentration increases the temperature required to evaporate the fluid into excitons increases also, up to a certain critical temperature, above which the liquid is not found.

There is a region in the phase diagram which is undetermined since the low concentration portion due to Timusk (1976) does not meet smoothly the extrapolation of the work of Thomas et al. (1973). The situation is further complicated by the fact that the curve representing the metal-insulator transition criterion as a function of density and temperature passes through this point, so it is possible that the form of the phase diagram is not simple, here.

Most experimental investigations of this region of the phase diagram, and, indeed, of most other properties of excitons and related species are performed using the recombination luminescence technique. In this method excitons etc. are generated and then the light emitted as they annihilate by the recombination of electron-hole pairs is observed. Since the exciton levels in the semiconductors lie just below the conduction band the photon energies observed are all of the order of the band gap energy. It is not possible to differentiate between recombination of excitons in different excited states, just one peak is observed. When observations are being made in the transition portion of the phase diagram, the peaks due to the different

Figure 2-2

Phase diagram of excitons in germanium (after T. Timusk 1976) The dotted lines indicate where the concentration of excitons has dropped by 50% due to thermal ionization (for two different electron lifetimes and recombination rates). The vertical dashed line indicates the Mott criterion. The curved dashed line is an extrapolation (using a Guggenheim plot) of work on the liquid phase.

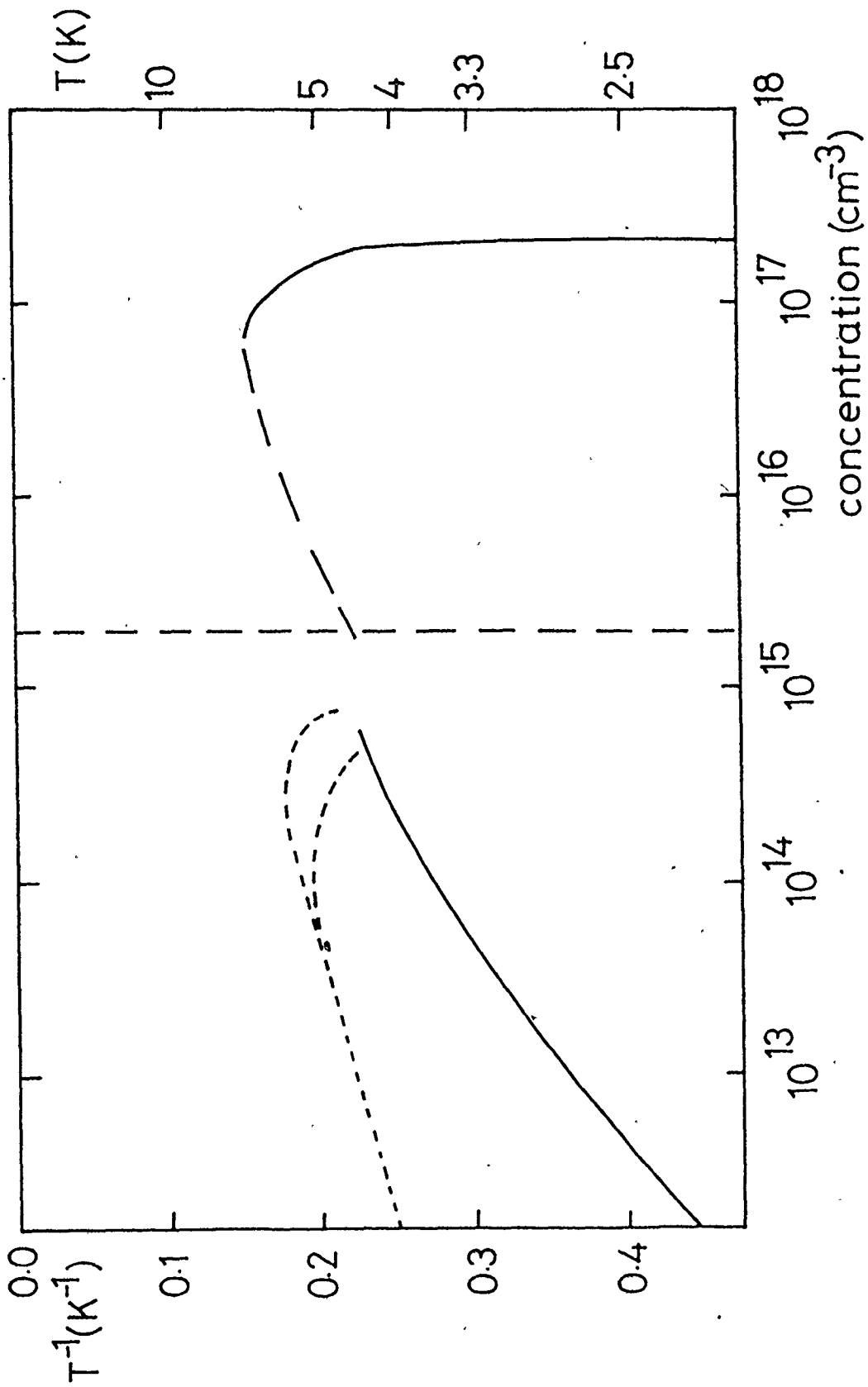
T(K)
10
5
4
3.3
2.5
10^{18}
10^{17}
10^{16}
10^{15}
10^{14}
10^{13}
concentration (cm^{-3})
0.0
0.1
0.2
0.3
0.4
$T^{-1}(K^{-1})$

Figure 2-3

Exciton experiments and formation. The upper diagram shows the energy ranges used in the far-infrared absorption and recombination luminescence techniques. The exciton energy levels are often regarded as lying just below the conduction band minimum. The lower diagram shows schematically the formation of indirect excitons. The electron absorbs a photon and is excited into the conduction band. It then interacts with a phonon, undergoing a change in k, and drops into an exciton level.

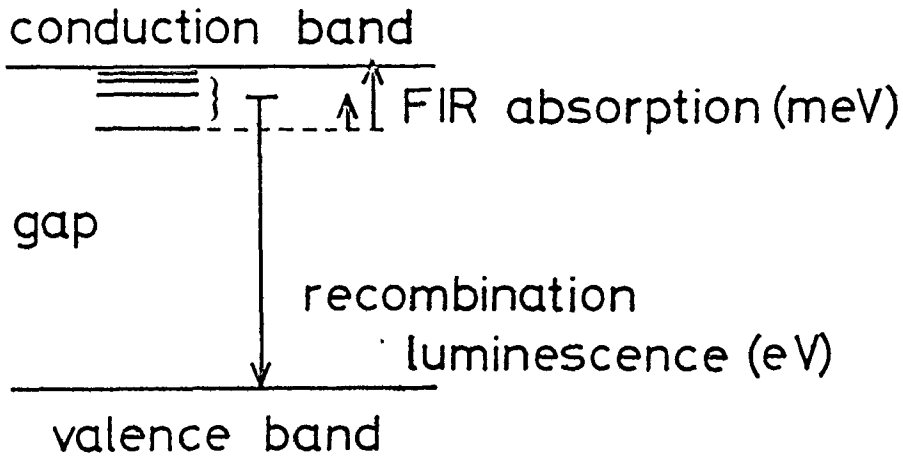
conduction band
FIR absorption (meV)
gap
recombination
luminescence (eV)
valence band

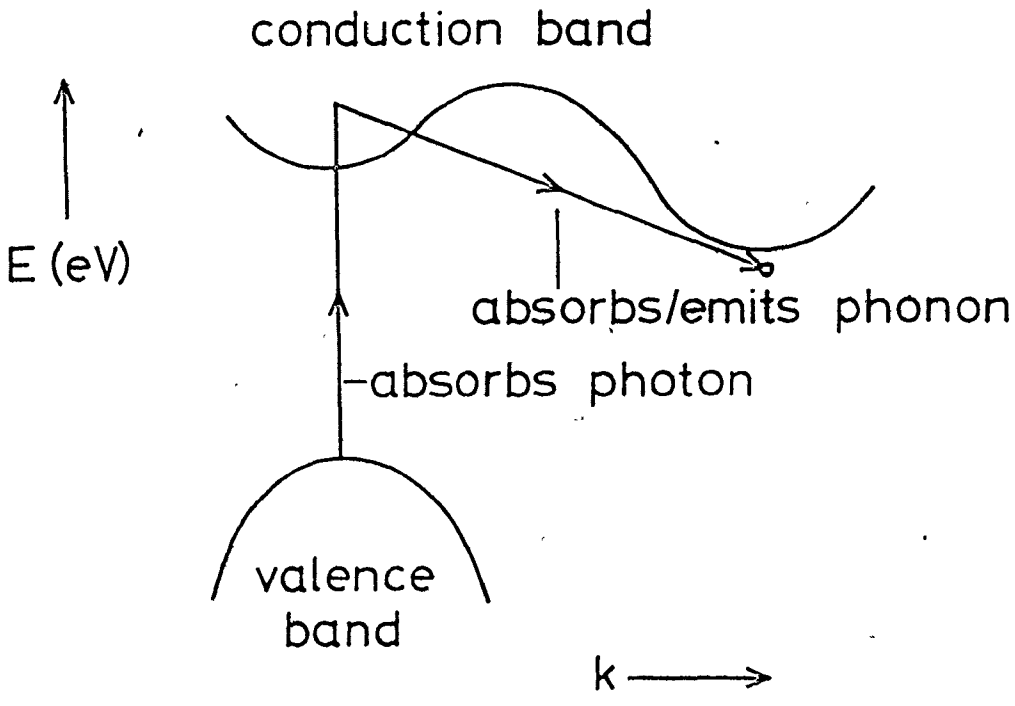
conduction band
E (eV)
absorbs/emits phonon
absorbs photon
valence
band
k

components (fluid, excitons and plasma) are to an extent superimposed.

The method used in this work is the absorption of far-infrared radiation. The excitons are generated continuously and far-infrared radiation is shone through them. The absorption spectrum is obtained by comparing the spectrum of excitons plus semiconductor with the spectrum due to the semiconductor alone. In these experiments transitions between the hydrogenic levels of the excitons can be observed, and the plasma, exciton, and fluid absorptions are clearly differentiated from one another.

The equipment used to perform the experiments will now be described.

(ii) Experimental Detail

Since excitons are only observed at low temperatures the sample is placed in a cryostat cooled with liquid ^{4}He to 4.2°K and pumped to 1.2°K. The cryostat also houses the detector (a germanium bolometer), which operates at 0.3°K, being cooled by pumped liquid ^{3}He. The excitons are created by shining continuous wave radiations from a Nd:YAG laser onto a spot on the surface of the crystal. The photons, which correspond to an energy of 1.17 eV - slightly bigger than the band gap energy in germanium (.74 eV) - excite electrons into the conduction band which form excitons with the holes in the valence band. The excitons form a hemispherical cloud of about one millimetre radius. The laser

radiation does not penetrate the sample deeply. Far infrared radiation is then shone along the same path, passing through the cloud of excitons, the sample, and filters and finally being received at the detector. The radiation is focussed by a polished cone, which like the light pipe, is made of brass. The laser is focussed by a lens outside the cryostat, to a spot of about 1.5 mm.

Two different samples were used in these experiments: a small rectangular one and a large irregular shaped one, both cut from the same crystal of germanium grown by Haller and Hansen (1974) donated by E.E. Haller. The concentration of electrically active impurities was $N_A - N_D < 2 \times 10^{11}$ per cc and the crystal was virtually dislocation free. The small sample ($\sim 2 \times 8 \times 5$ mm) which was dislocation free, was obtained from experiments of G. Zárate. The large one had small dislocations at one edge (visible by the etch pits they produced), well away from the region containing the excitons. This was cut using a diamond grit wafering blade, the cut face being polished down with successively finer grades of carborundum paper and finally 6 μ then 1 μ diamond paste. The crystal was then etched with CP4*. The etching was repeated using CP4A (CP4 without the bromine) every few experiments, to improve surface quality, as this leads to a better absorption of laser power.

---

*(hydrofluoric acid 50 parts: acetic acid 50 parts: nitric acid 80 parts: liquid bromine 1 part)

Figure 2-4

The sample holding probe in the cryostat. This schematic diagram shows the relative position of the various parts described in the text. The light pipe bending apparatus, lens and aperture are described in chapter four.

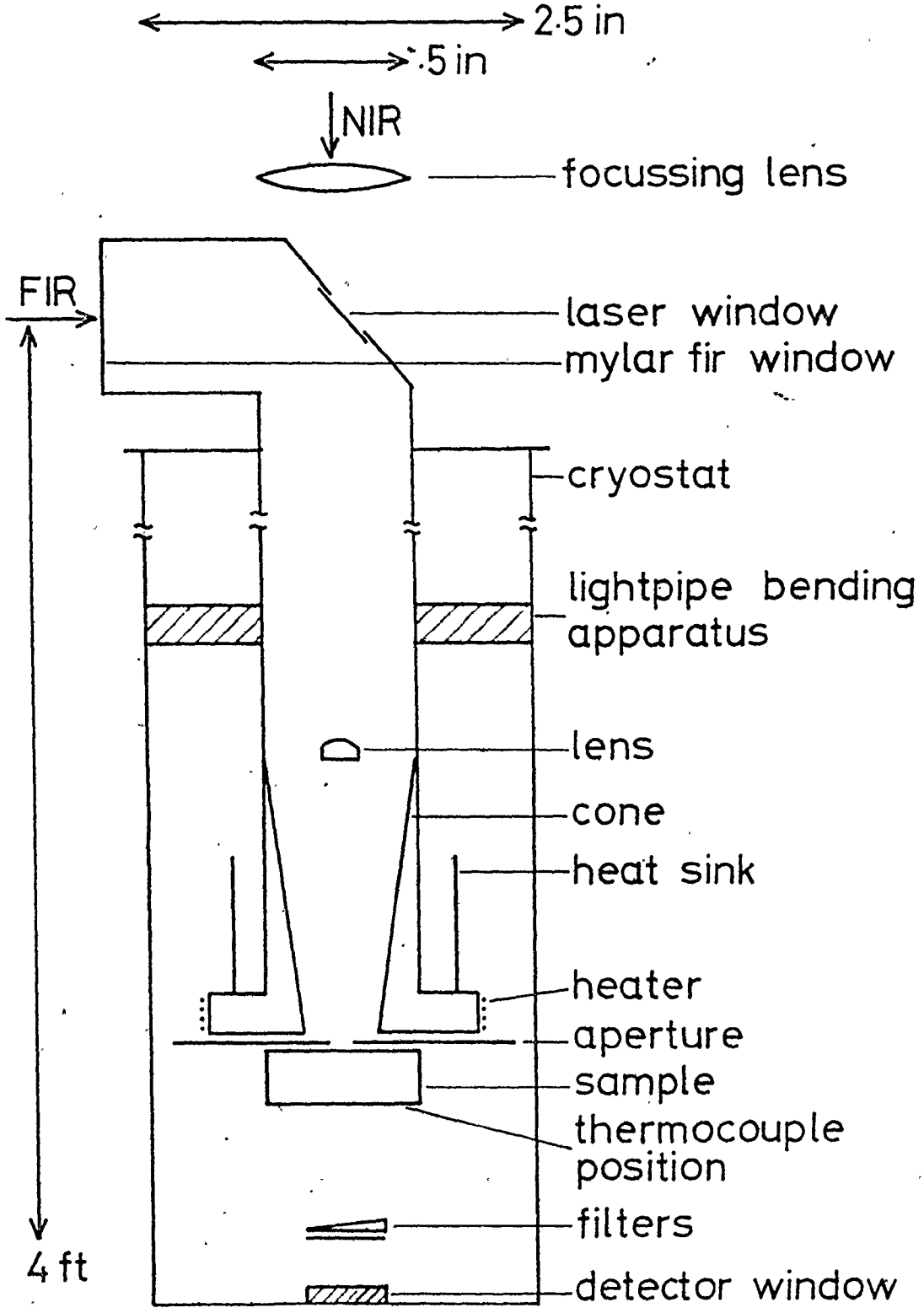
2.5 in
.5 in
NIR
focussing lens
FIR
laser window
mylar fir window
cryostat
lightpipe bending apparatus
lens
cone
heat sink
heater
aperture
sample
thermocouple position
filters
detector window
4 ft

To obtain higher pumping powers the single mode aperture normally in place in the laser was removed. The multimode power available is four times greater than the single mode power, but the beam divergence is greater, so an additional lens was required to focus the laser to a spot of $\sim$ 1 mm. When this lens was in position an additional means of lining up the optical elements was required: the light pipe bending apparatus. This will be described further in chapter four.

The filters were used to restrict the wavelength range of the radiation reaching the detector so that extra detector heating, and the need to study the full range to avoid aliasing in the Fourier transform, were avoided. The wavelength range varied according to the concentrations being studied, more details will be given in the corresponding chapters.

The liquid ^{4}He was contained in a separate can surrounding the insert containing the light pipe and sample. The whole insert was vacuum tight and was evacuated thoroughly before an experiment to avoid adsorption on the light pipe walls of any absorber of far-infrared radiation, e.g. water. During the experiment it was let up with exchange gas (^{4}He) to remove heat produced in the sample by the laser and generated when the sample was heated to change the temperature. The sample was pressed against the copper block holding the heater and heat sink, with indium pads between the block and the sample for good thermal contact. The sample temperature was measured with a thermocouple.

The far-infrared radiation was in the form of an interferogram generated by an ordinary Michelson interferometer or a polarising interferometer (made by C. Zárate). The difference between the two interferometers is that the beam splitter of the Michelson is replaced by a wire grid in the polarizing interferometer, and an input polariser and polarising chopper are added. The configuration of the mirrors is the same in the two cases. The mylar beam splitters used in the Michelson interferometer become very inefficient at long wavelengths whereas the polarising beam splitter is almost 100% efficient. This means that data can be obtained at much lower energies with the polarising spectrometer, being limited then by the lamp spectrum. The higher energy spectra are better obtained with the Michelson, since the polarising spectrometer becomes inefficient as the radiation wavelength approaches the beam splitter wire spacing. The range used was from about 1 meV to 10 meV in our experiments. Spectra were taken at up to 20 meV using the Michelson, the limit being due to filters in the cryostat.

Normally a chopped DC far-infrared signal would be detected with the moving mirror being stepped through the interferogram but the Michelson in this laboratory uses the rapid scan technique, where the mirror is moved continuously at fast speed through the interferogram. No chopper is needed, the interferogram changes sufficiently fast to be detected as an AC signal. A special oil-lubricated bearing was used in order that the mirror move smoothly and regularly (Timusk and Lin, 1980).

The signal from the detector representing the interferogram is amplified (Michelson), or detected using a phase sensitive detector at the chopping frequency (polariser); the output from these passes via an analogue to digitial converter or voltage to frequency converter to the computer. The computer performs a fast Fourier transform of the interferogram and displays the spectrum, producing a plot if required. The acquisition of data, control of motor-translation and determination of mirror position as well as the production of spectra from interferograms are all regulated by an extensive, continuously developed and improved computer program. The user determines the number of spectra to be averaged together by examination of the spectrum and input parameters such as resolution cut-off etc.

The absorption spectrum is obtained by taking the ℓn of the ratio of the spectrum obtained with the pumping laser switched off (I_0), i.e. the germanium only, to the spectrum of germanium plus excitons (I). Since $I = I_0 e^{-\alpha d}$ where αd is the absorption, d being the distance in the excitons through which the far-infrared radiation passes, we have

$$\ell n\left(\frac{I_0}{I}\right) = \alpha d \ .$$

The absorptions, αd, studied in this work varied from 0.01 to approximately 4 or 5 but at the low concentration end of the scale data taken at $\alpha d = 0.01$ were found to have a large scatter,

Figure 2-5

Energy and signal flow diagram.

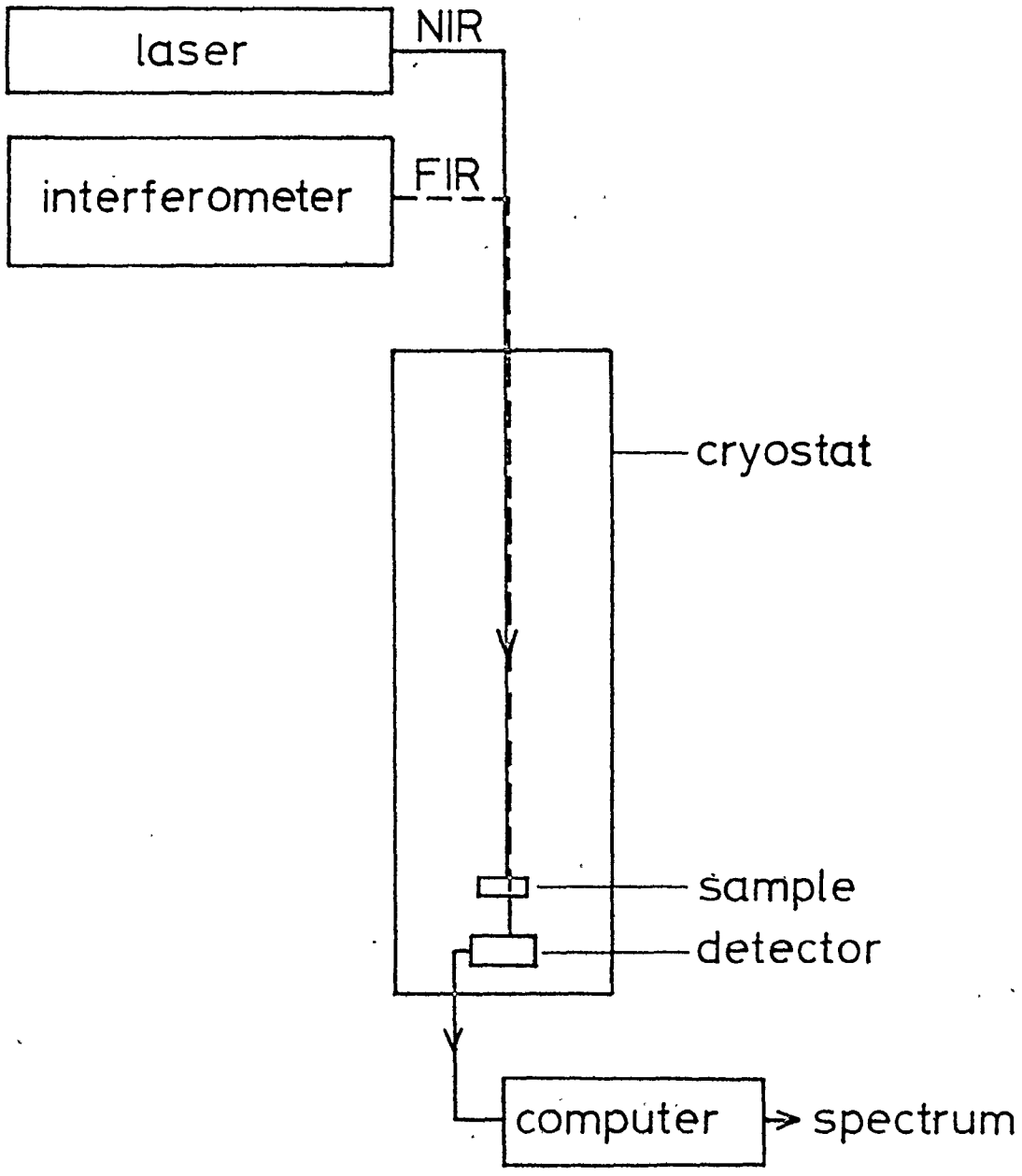
laser
NIR
interferometer
FIR
cryostat
sample
detector
computer
spectrum

here only 1% of the light was absorbed. At $\alpha d = 0.1$, corresponding to 10% absorption, the scatter was greatly reduced. The type of measurement being made was very sensitive to small changes in experimental conditions e.g. slight temperature changes. For the high concentration measurements, at absorptions greater than 3 (5% transmission) or 4 (2% transmission) there was so much noise at the peaks that these could not be determined. Obviously when the transmitted signal is of the order of the noise on the spectrum the absorption cannot be distinguished from 100% (αd very large).

This description of the experimental setup is just a brief introduction: for fuller details the theses of G. Zárate (1981) and H. Navarro (1979) may be consulted. "Introductory Fourier transform spectroscopy" by Bell (1972) gives a good deal of the spectroscopic detail; "Far-infrared Spectroscopy" by Möller and Rothschild (1971) is also useful.

Some parts of the experimental system will be discussed in more detail in chapters three and four.

CHAPTER 3

THE PHOTO-IONIZATION CROSS SECTION OF EXCITONS

(i) Introduction

In 1976 Buchanan and Timusk published a paper on the far-infrared absorption of excitons in germanium, (Buchanan and Timusk, 1976). A small part of this dealt with the region of the spectrum which corresponds to photo-ionization of the excitons. By comparison with the hydrogen atom theory they expected to see a variation of absorption with frequency that varied as the $-\frac{8}{3}$ power: $\alpha d \sim \nu^{-x}$, where $x = \frac{8}{3}$. The value they obtained was $x = 2.6 \pm .5$, which is in agreement with the theory.

The purpose of this part of the research was to try and confirm this measurement, which was the result of just one experiment, and also to see if there was any variation of x with concentration of excitons.

Surprisingly the new results were in disagreement with that of Buchanan and Timusk. Also, a slight variation of x with concentration was observed. No other authors have subsequently investigated this particular point.

In the following sections of this chapter a brief summary of the hydrogen calculation, details of any special experimental requirements, and a discussion of the data, including a comparison to the hydrogen, and other, models will be given.

(ii) Simple Hydrogen Theory

When electromagnetic radiation is absorbed by an atom, the electron makes a transition between two energy levels. These levels may be discrete or continuous, or, as in the case under consideration here, one of each: the exciton absorbs a photon of energy $\hbar\omega$ and makes a transition from the bound state E_n to a state in the continuum of energy W, where

$$W = \hbar\omega - I \ .$$

I is the binding or ionization energy and is equal to $- E_n$.

The absorption of energy by a hydrogen-like atom from the incident radiation is proportional to a quantity called the cross-section, σ, where

$$\sigma = \frac{2\pi e^2 \hbar^2}{m^2 c \nu} |D|^2 \ .$$

D is the matrix element for the transition between the bound and free states, all other symbols have their usual meaning. The unit of σ is area. The cross-section is simply related to the absorption coefficient α:

$$\alpha = N\sigma$$

where N is the number per unit volume of atoms in the ground state. (Of course these quantities can be defined for any bound state, but only the ground state is being considered here.) The experimental quantity obtained as discussed in chapter two is $\alpha d = \ell n(I_0/I)$. In order to compare the theory with experiment the matrix element has to be evaluated, and the dependence of

σ on ν obtained. In general exact expressions for σ cannot be obtained and various approximations have to be made.

The hydrogenic wave functions are used for the initial and final states. These are correct in so far as the exciton may be considered to be a one electron atom held together by a Coulomb potential. The masses of the two constituents are in a completely different ratio to those in hydrogen. The only effect this will have on the result will be to reduce the depth of the ground state (Bethe and Salpeter (BS) 1957, §5). The electron mass must be replaced by the reduced mass $mM/(m+M)$ where M is the nuclear mass. Then all energy levels are multiplied by a factor $M/(M+m)$. This effect is small in hydrogen where M is much larger than m, but much larger in the exciton. For germanium the masses of the heavy and light holes are approximately 0.3 and 0.04, and the electron mass 0.1* (Brinkman and Rice (1973)). (The value of the binding energy is also reduced by the fact that the germanium lattice is a dielectric, and screens the attractive interaction.) This will affect the magnitude of σ, but not its dependence on frequency. The effects on fine and hyperfine structure are profound, c.f. positronium ($M = m$) (BS §23), but this does not concern us in the present calculation.

The bound state of the electron is treated non-relativistically and its spin is neglected. If $W \ll mc^2$ the continuum state may be treated this way also. The wavelength of the incident radiation (0.01 to 1 cm) is much larger than the

*regarding the mass of the free electron as unity.

exciton ($\sim$ 100 Å) so the electric dipole approximation may also be used to simplify the matrix element, which is given by

$$D = \frac{m\nu 2\pi}{h} \int u_W^* \, x \, u_b \, d\tau .$$

In this approximation u_W and u_b are the free and bound wavefunctions respectively, integrated over configuration space, x is the polarization direction of the photon.

If the final energy, W, of the electron was large compared to the ionization energy we could use plane wave states for u_W (the Born approximation), but σ_d was measured quite close to the ionization energy. In this case the electron has a small final kinetic energy and is still influenced by the Coulomb field of the nucleus. The exact hydrogenic continuum wavefunctions must be used, which makes the calculation much more complex. It is performed in BS §71.

The final result is that the cross-section goes as $\nu^{-8/3}$ very near the ionization onset, ν^{-3} when $W \sim I$, and $\nu^{-7/2}$ when W is much larger, the latter corresponding to the Born approximation result.

The result is expressed conveniently by Clayton (1968) as

$$\sigma \propto \frac{g(\nu, n, \ell, z)}{\nu^3}$$

where g is called the Gaunt factor. These factors may be found in the literature. For hydrogen-like atoms they are nearly constant and near unity near the threshold.

(iii) Experimental Details

The experimental setup for the low to medium concentration investigations was just the basic system described in chapter two. The filters used to restrict the spectral region were sodium chloride together with black polyethylene. The black polyethylene cut out the higher energies where NaCl is transparent and the NaCl further lowered the cutoff to 170 cm^{-1} or about 21 meV.

It was comparatively simple to align this system so that the laser beam hit the required spot on the sample. The cryostat had a plumb-line attached which pointed to the centre of a target when the cryostat was vertical, and the vertical alignment of the laser could be checked in a similar way, and this was usually all that was necessary.

The main difficulties occurring in these experiments, particularly at low concentrations (absorptions of 1 to 10%) were slow fluctuations in the signal level caused by temperature fluctuations in the sample or detector. These were extremely undesirable since they caused the laser on signal, or the laser off signal, I_0, to be multiplied by a constant gain factor which had the effect of shifting the baseline of the spectrum, $(\ell n(I_0/I))$ up or down by a constant amount. When the logarithm of this spectrum was plotted, this effect appeared as a change of slope, x, thereby mimicking the effect under study. Because of this the temperatures of the sample, the detector, and sometimes the

^{4}He exchange gas were monitored continuously.

The sample temperature was measured with a thermocouple observed on a digital voltmeter and the heater current was adjusted to keep this constant, since the sample temperature changed when the laser was switched on and off. The sample was held against a copper block with a cooling fin attached, using indium pads between the block and sample for good thermal contact. A larger sample was used for later experiments. This showed greater temperature stability.

The detector temperature was monitored using a chart recorder. When the data were being taken the chart was marked so that upon later examination data obtained when the detector temperature was unstable could be rejected. The detector temperature was found to change if the sample temperature was altered to any extent, by design or because of an increase in laser power. Since the thermal contact between the sample chamber and detector was not very good, time was allowed for the temperature to stabilize. This effect could also be seen by monitoring the exchange gas pressure, as an extra check. When the ^{4}He level became low compared to the detector, the temperature would exhibit spikes, and the experiment would be terminated at this point.

The detector temperature could also be changed by a change in the level of incident radiation, such as that produced when a high concentration of excitons absorbs a large fraction

of the far-infrared radiation giving a potential temperature difference between I and I_0 data. This effect could be reduced by having an aperture at the sample small enough so that the quantity of radiation in either case would be sufficiently small so that the detector temperature was not disturbed. No effects like this were observed on the temperature monitor, however, therefore the aperture size was deemed to be satisfactory.

The biggest source of random noise was fluctuations in the laser power. These were minimized by keeping the laser in good working order: keeping the mirrors clean and aligned, and ensuring a sufficiently fast flow of clean cooling water.

Many spectra were averaged to produce the final ad spectrum, and the spectrum was observed as the averaging took place. If a sudden large change in the average occurred the spectrum was rejected since a spurious I_0 or I spectrum had been added in.

(iv) Experimental Data

An example of the experimental data is shown in the diagram. This is an example of a higher concentration ad spectrum and is therefore of good quality. The sample temperature was 6.5°K and the laser power incident on the sample was approximately 1 mW. The resolution was 0.3 meV. Five I_0 spectra and five I spectra were averaged together to produce this ad spectrum. Each of the I and I_0 spectra consisted of the Fourier transform of the average of fifteen interferograms. What might appear to

Figure 3-1

A typical sample of experimental data.

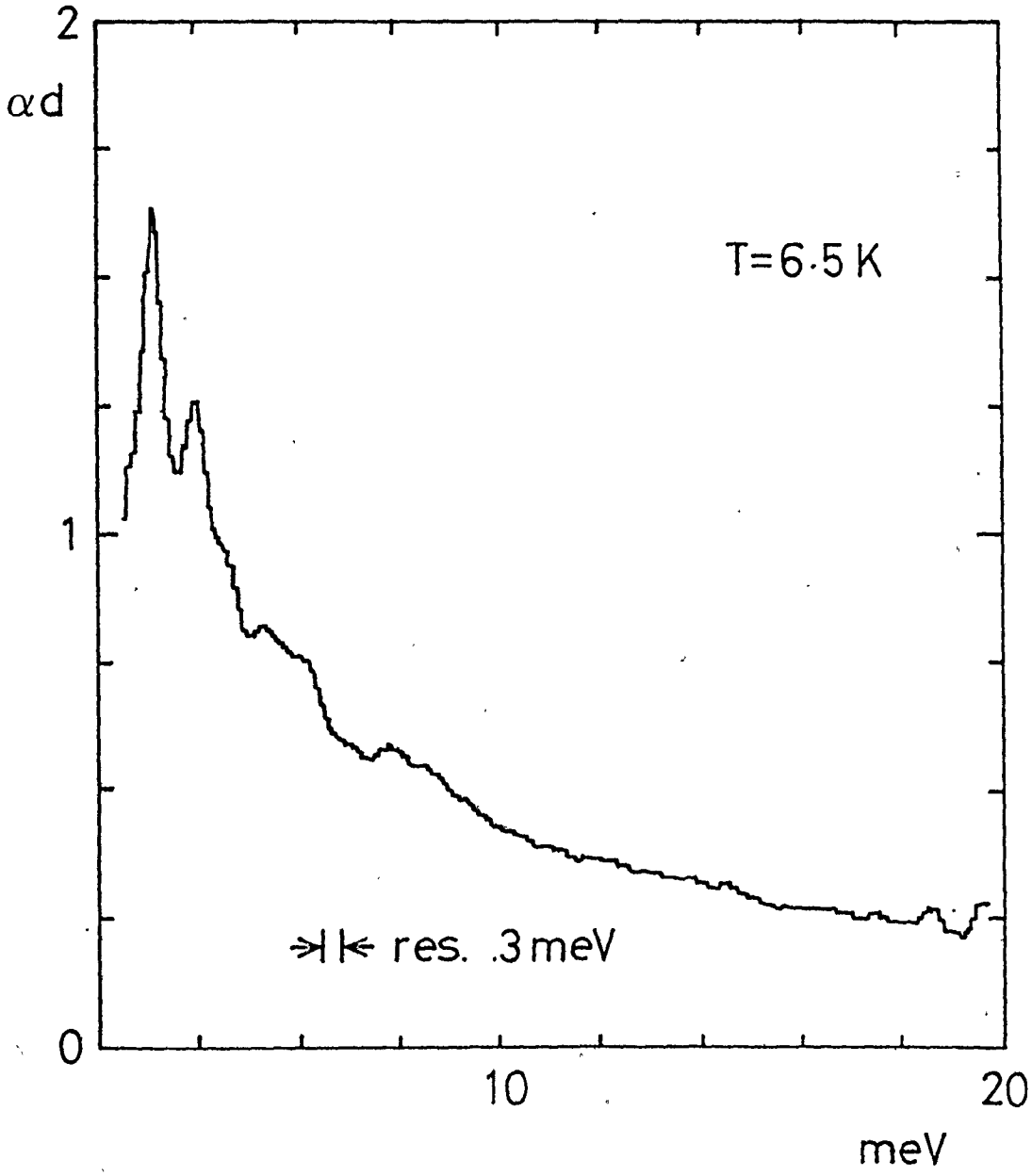
2
αd
T=6·5 K
1
⇒I⇐ res. .3meV
0
10
20
meV

be structure above 4 meV, is noise. The concentration of excitons is 1.3×10^{14} cm^{-3}. The concentration is determined by the strength of the absorption peak at 3 meV following the procedure of Timusk (Timusk, 1976). It is given by

$$n_{ex} = 0.09\ell n(I_0/I) \times 10^{15} \text{ cm}^{-3} .$$

About 80% of the far-infrared radiation at this frequency was absorbed. There is still an absorption of about 15% at the high energy tail.

Twenty-three αd spectra of this kind were obtained over six separate experiments, at concentrations ranging from 2.3×10^{12} cm^{-3} to 2.3×10^{14} cm^{-3}, and temperatures ranging from 3.5°K to 7.5°K. They were analysed by taking a set of αd versus energy points and performing a linear least squares fit to the logarithms of these values. In the lower concentration data noise appeared on the high energy end of the spectrum to such an extent that it was necessary to restrict the range to 4 - 12 meV. The slope of this fitted line is the quantity x under investigation. The values of x obtained were between 0.84 and 2.1.

No obvious correlation between x and temperature seemed to exist. The values of x were plotted on a phase diagram in order to examine whether they were correlated with the distance away from the boundary of the phase transition between excitons and electron-hole fluid, but again the result was negative. If there are correlations of this kind they are hidden within the

scatter on the data. For this reason a diagram of this is not shown.

A plot of -x against concentration showed that the magnitude of x definitely decreased with concentration. The approximate size of the experimental error may be seen from the scatter on the data. (No other method of determining error was used.) The line drawn through the points is a least squares fit, the slope is 0.12. The value of x predicted by the hydrogen theory (-8/3 or -2.7) is significantly higher than all the data points. It is not possible to obtain data at any lower concentration to determine whether or not x does eventually approach this value.

The next diagram shows curves of $\nu^{-1.5}$ and $\nu^{-8/3}$ and the difference of the two. This shows how a shift with respect to the baseline could distort the value of x, because the difference function is very slowly varying at energies higher than 1.5 × (ionization energy). A plot of ν^{-1} and ν^{-1}-(constant) is also shown to illustrate this point. (See also discussion in section (iii) of this chapter.)

As stated in section (iii), however, great care was taken to eliminate data that would be subject to such shifts. It would also be extremely unlikely for all the shifts to be such as to produce a decrease in x, since they would randomly affect I_0 or I, and finally they would not explain the concentration dependent change in x.

Figure 3-2

Plot of -x vs concentration. The line is a least squares fit to the data. The value expected for a hydrogen-like atom is shown.

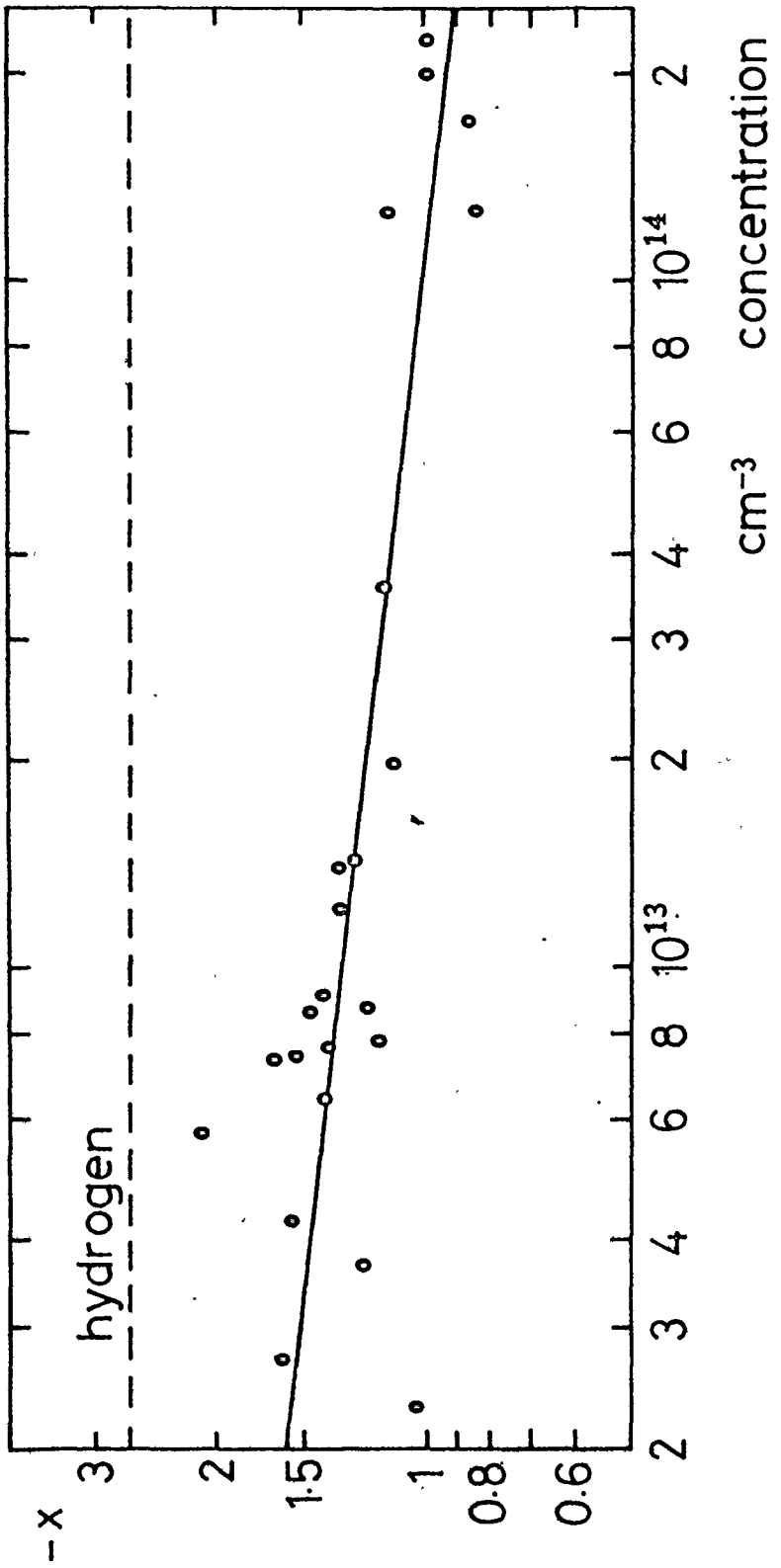
hydrogen
-x
3
2
1.5
1
0.8
0.6
2
3
4
6
8
10^{13}
2
3
4
6
8
10^{14}
2
cm^{-3}
concentration

Figure 3-3

The effect of baseline shift on x. Part (a) shows how a constant additive background might distort x in the ν^{-x} dependence of the photoionization, since the difference between the two plots ($\nu^{-1.5}$-$\nu^{-2.7}$) is nearly constant for much of the range. Part (b) shows the change in slope of a logarithmic plot when a constant is subtracted from the data (c was 20% of the value of ν^{-1} at 4 meV).

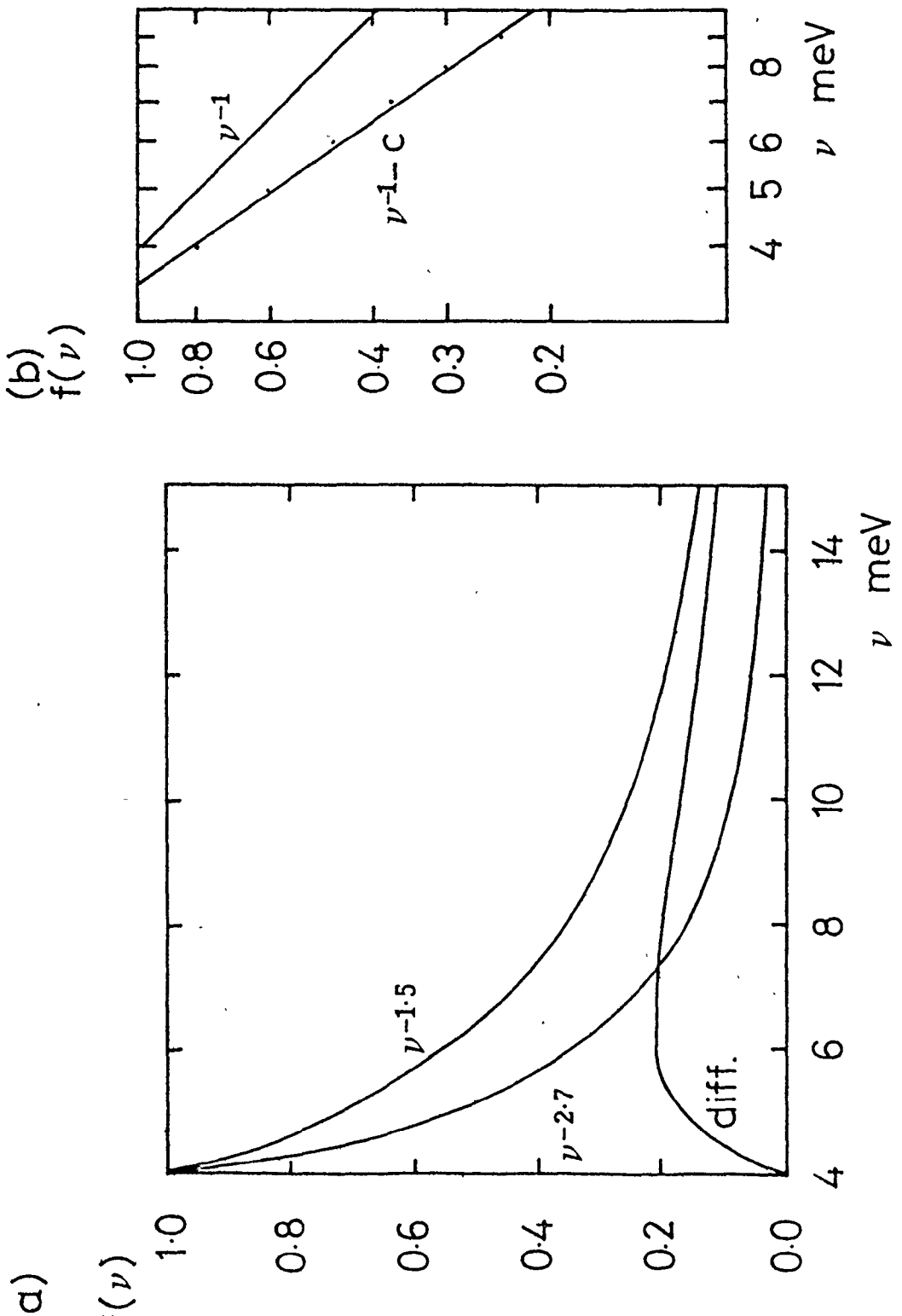
(a)
f(ν)
1·0
0·8
0·6
0·4
0·2
0·0
4
6
8
10
12
14
ν meV
ν^-1·5
ν^-2·7
diff.
(b)
f(ν)
1·0
0·8
0·6
0·4
0·3
0·2
4
5
6
8
ν meV
ν^-1
ν^-1_c

Any concentration dependent shift due to the size of the aperture would act to increase, rather than decrease, the apparent slope. For a large aperture the grain of the detector would increase as the concentration of excitons increased, since less radiation would fall on the detector and its temperature would be lowered. We have then

$$\ell n(I_0/I_x c) = \ell n(I_0/I) - \ell n\ c$$

where c is a gain factor greater than one in this case. It has been seen that subtracting a constant from the spectrum increases the apparent slope.

The concentration dependence of x, and deviation of x from -8/3, must therefore be taken to be a real deviation from the hydrogenic theory.

(v) Discussion of Results

The results show clearly that there is a large discrepancy between the hydrogen and the excitonic ionization behaviours. There are many differences between a hydrogen atom and an exciton in germanium, but whether any of these differences are sufficient to cause the effects seen has not been determined theoretically.

Considering the electron and hole as particles with the properties given by the band structure we see that the following differences exist. The mass ratio of the electron to hole is very different to that of the hydrogen electron to nucleus. The

variation of the energy of the constituent particles with wave-vector is parabolic and isotropic in hydrogen: in the exciton the light hole constant energy surfaces are nearly spherical, the heavy hole ones less so, and the electron surfaces are extremely elongated (masses in the ratio of, 20:1) ellipsoids of revolution. The strength of the interaction between the particles is less by a factor of ε_0 (the static dielectric constant) in the exciton case. There is a spin-orbit coupling between the spin of the hole and the angular momentum of the exciton which is 860 times bigger than spin-orbit coupling in the hydrogenic case (Navarro 1979). It is zero for the s states in hydrogen. (The spin orbit effect due to the proton in hydrogen is smaller than that due to the electron by the ratio of their masses, about 5×10^{-4}.)

The effect of many of these differences has been calculated, as is reviewed in the thesis of H. Navarro (Navarro 1979).

The spin orbit coupling has the effect of shifting the ground state. The exciton Hamiltonian, which can be divided into terms of different symmetry, spherical, cubic and d-like (as described in chapter two), includes the spin orbit effect in the spherical term.

The anisotropy of the valence band is included in the cubic symmetry term. Once again the effect is to shift the ground state energy.

In indirect semiconductors the large axial, or d-like term resulting from the anisotropy of the electron masses shifts and splits the ground state. The exciton wavefunction, which was originally summed over the light and heavy hole states, now gives the lighter exciton as the lower, more tightly bound, ground state for a stationary exciton. As the momentum of the exciton increases, however, the light and heavy states interact and repel one another, and the situation is reversed (Kane 1975). From a hydrogenic point of view we would simply expect the light hole exciton to be less tightly bound than its heavy counterpart, and both to be much less tightly bound than hydrogen (see section (ii)).

A calculation performed for excitons with highly ellipsoidal bands (Shinada and Sugano 1966), in effect a "two-dimensional" hydrogen atom, with the heavy mass tending to infinity, predicts that the absorption to the continuum will show a decline and then a peak after the ionization threshold, followed by a slow decline.

In the effective mass method the use of the static dielectric constant in reducing the strength of the Coulomb interaction merely scales the depth of the energy levels and the spatial extent of the exciton. This is really valid only for an electron and a hole separated by large distances. The screening then depends on the polarization of the lattice ions (excitation of optical phonons). As the separation between electron and hole decreases the valence electron polarization screens the

Coulomb interaction, with the high frequency dielectric constant, since the rotation frequency of the electron and hole around each other has increased. As this increases still further (electron and hole now separated only by the order of lattice constants) the screening will become effectively zero (Madelung 1978).

Thus far the differences between the excitons in germanium and hydrogen have been listed, and the theoretical treatment of them has been described. This must now be applied to account for the experimental observations of section (iv), a task which will be attempted qualitatively here.

The effective mass theory has been used to calculate an energy level scheme which has been compared quite successfully with experiment. (See, for example, Navarro (1979) who confirmed the comparisons of other researchers and also identified new transitions between levels.) This does not specifically enlighten the present situation however.

Some features due to the anisotropy of the electron mass have been observed, namely the decline and increase of the continuum absorption (Buchanan and Timusk 1976) predicted by Shinada and Sugano. The data taken for this thesis also seemed to exhibit this effect. For example, in the sample given two "peaks" can be seen. One, centering at 3 MeV, consists of the peaks due to the transitions between discrete levels of the exciton, which cannot be seen separately at the resolution used. The other, at 4 meV, could be attributed to the aforementioned effect. A

decrease in absorption is clearly seen between them. This was also seen in other, mainly high concentration, data, because the higher signal to noise ratio meant that higher resolution could be used, and also that less noise would be present to obscure the peaks if they were resolved. Some features of the data appear to be described by this theory but again the specific frequency dependence of absorption could not be compared.

The problem of the frequency dependence of transitions to the ionization continuum has been examined for impurities in semiconductors. Impurities behave like excitons to a certain extent. The conduction electrons from donor impurities occupy levels just below the conduction band although the impurity atoms are fixed. A hydrogen like model has been applied to these systems and found to describe the ionization frequency dependence incorrectly.

G. Lucovsky (1965) suggested a model which would account for this. Stating that the wavelength dependence of the photo-ionization cross-section depends on the potential between the electron and the impurity he took as a potential a delta function at the origin (the ion-core potential), the strength being determined by the binding energy of the impurity. The wavefunction used was a delta function potential well ground state $\frac{1}{\sqrt{2\pi a}} \frac{e^{-r/a}}{r}$ where a is the equivalent of the Bohr radius. The exact form of the short range potential does not affect the frequency dependence of the cross-section. His calculation

showed a frequency dependence of $\nu^{-1.5}$ and a maximum of absorption at twice the ionization energy, starting from zero at the ionization energy. If the delta function is combined with a long range Coulomb potential, which would be necessary for the exciton, the absorption is still enhanced at higher frequencies and the absorption maximum varies between one and two times the binding energy.

This could usefully be applied to the data at hand, if a reason could be found to justify the use of stronger potential at short range. As discussed above, if the dielectric constant varies with the separation of the electron and hole, becoming unity at zero separation, the potential there could be greatly enhanced for an electron which approaches closely: this would apply more to the 1s electron than any other. If, as a crude estimate, the new wavefunction consisted of a 1s wavefunction of full strength up to one lattice spacing away from the hole in the central cell, and a dielectric constant reduced wavefunction outside this radius ($\psi = (\pi a^3)^{-1/2} e^{-r/a}$ where $a \rightarrow a/\varepsilon = a/15.8$, a being the exciton Bohr radius), one can see how the use of a delta potential wave function in this region might not be unreasonable, since the $\frac{1}{r}$ factor in the latter makes the wave function large at small separations. Pictorially this looks like a large spike at the origin.

The central cell model, then, could be used to explain the large difference between the hydrogenic and observed ionization cross-section energy dependences. At the lowest concen-

trations measured the excitons are separated by a distance of the order of 30 exciton radii. The value of the power of the cross-section frequency dependence, x, at this point may be taken to be the value for an isolated exciton. This value was found to be 1.4(± 0.2).

At higher concentrations x is weakly dependent on concentration, but the central cell model contains nothing to explain this effect. Indeed, a value below 1.5 cannot even be obtained.

Attempts to explain the concentration dependent effect in terms of a varying balance of light and heavy excitons in the population were unsuccessful. A calculation of the cross-section for a transition in which the mass of a particle changed showed that the new cross-section was merely scaled by the mass ratio. The frequency dependence did not change.

As concentration and temperature increase the number of heavy excitons increases. The heavy exciton state corresponds to the more weakly bound state, which has a large Bohr radius, and thus penetrates the central cell less therefore behaving more like hydrogen. Thus if an effect of this type was observed (which it was not, as a function of temperature) it would lead to an increase, rather than decrease, of x.

A possible explanation is that the spectrum is distorted by absorption due to the presence of other species such as biexcitons, trions or plasma. The effects of these are explored in the work of the next chapter.

CHAPTER 4

EXCITONS AT HIGH CONCENTRATION

(i) Introduction

As the density of excitons in a semi-conductor increases, at low temperatures, the exciton gas condenses into a metallic fluid of electrons and holes. This fluid can coexist with excitons at a temperature, which varies with concentration, of 2 - 6.5°K or lower. This chapter attempts to examine what happens as the density is increased, above this temperature. The excitons may possibly all ionize, forming an electron-hole plasma, as discussed by Rice (1974). This type of transition was originally proposed by Landau and Zeldovich (1943). This may take the form of a metal-insulator transition.

The metal insulator transition was described by Mott, in 1949, who imagined an array of hydrogen-like atoms with a lattice constant that could be varied. For small values of the lattice constant the material would be metallic, and for large values, an insulator, (Mott 1974). This can be observed in heavily doped semiconductors as the doping is varied. The density criterion for this transition to occur in excitons in germanium is $n = 1.6 \times 10^{15}$ cm^{-3} (Thomas et al. 1973).

The phase diagram (see chapter 2) shows the density criterion and curves indicating the region where the exciton con-

centration is reduced by 50% due to ionization (Timusk 1976). As the density of the excitons increases the ionization curve will be moved to lower temperatures due to a reduction of the exciton binding energy by screening in the plasma (Clayton 1968). The two curves are obtained using different electron lifetimes and exciton recombination rates.

T.M. Rice (Rice 1974) suggests the possibility of two peaks on the phase diagram corresponding to separate electron-hole fluid to exciton transitions and fluid to plasma transitions. This would imply a discontinuous change in the nature of the excitonic matter as the density increases.

Experimental work done in this field is ambiguous. Some workers claim to have observed a metal-insulator transition take place (e.g. Balslev and Furneaux (1979) in Ge; Shah, Combescot and Dayem (1977) in Si) and others (Thomas and Rice 1977) claim that only excitons, biexcitons and trions are observed above the critical density, rather than a plasma.

It is possible that this concentration is higher than can be achieved and observed by our equipment. The concentration is always subject to uncertainties in the parameters used to estimate it; in addition , at high concentrations, the absorption of close to 100% of the far infrared radiation prevents estimation of the concentration in the usual way (Timusk 1976) since it prevents determination of spectral features.

The next section (ii) describes the experimental proce-

dures undertaken to try and increase the concentration of excitons to levels not previously attained with the equipment. Section (iii) presents the results of the far-infrared spectroscopy and section (iv), the discussion of these.

(ii) Experimental Details

There are two main classes of methods of increasing the concentration of excitons in a sample of germanium, assuming that the given sample is as pure, dislocation-free and clean as possible: firstly, increasing the absorbed laser power, and secondly, modifying the sample. The second class was found to be less effective in terms of increase in concentration. More success was achieved with the first.

Two methods were tried in the second class: application of uniform stress and application of non-uniform stress. The application of non-uniform stress has been used successfully in luminescence experiments on electron-hole fluid to confine the fluid to a small spatial region of the sample (Markiewicz et. al. 1977). Droplets, excitons and free carriers migrate towards regions of maximum strain. If the stress is applied in the <111> direction in germanium, only one such region is obtained. The maximum lies along the line of application of the stress at a distance from the point of application that depends on the radius of curvature of the applicator. The magnitude of the strain well produced depends on the pressure applied. This also affects the diameter of the well. The effects produced have been calculated

by J. Hertz (1881) for solids of isotropic elastic properties. The properties of germanium being anisotropic, the problem becomes too complex to solve analytically. Markiewicz et al. performed numerical calculations for a germanium sample with a nylon applicator.

As a trial, a brass applicator with a spherical surface of radius of curvature approximately three inches was used and an experiment performed using the stress apparatus of G. Zárate (Zárate 1981). No significant increase or decrease in concentration was obtained when stress was applied. The position of the well was not known, but if it was outside our viewing aperture the exciton concentration would be expected to decrease as stress was applied. It is possible that excitons are not confined as readily as fluid. In the absence of a large effect, however, it was decided not to pursue this line of endeavour.

Uniform stress was used by I. Balslev and J.E. Furneaux (1979) in a luminescence experiment, since the application of a sufficiently high stress in the <111> direction reduces the concentration of excitons required to obtain the metal-insulator transition by a factor of three. (That these conditions of stress would be satisfied was known by comparison to the experiments of G. Zárate). While this would not be sufficient to observe a sharp transition, since in our case the concentration would still not be high enough, it was hoped to see effects of a gradual transition, if such took place, perhaps in the form of a plasma component appearing in the absorption spectrum at

temperatures below those where ionization should set in. Normally, a plasma would be observed in the region below 2 meV, but when the stress was applied the exciton peaks shifted to lower energies and dominated this region. The behaviour of the spectrum in the region where transitions to the continuum should take place appeared to be quite different to the non-stressed case, but this could not be related to any of the expected signs of the metal-insulator transition, such as the appearance of a plasma, or broadening of the exciton lines (Timusk 1976).

In view of the difficulties encountered with the stress methods, it was decided to try and produce a higher concentration of excitons by increasing the laser power absorbed in the sample. This would have two advantages: firstly, the effects of improving the power absorption were expected to be bigger than those produced by stressing the sample and, secondly, any effects seen in the absorption spectrum which were due to the metal insulator transition would not be complicated by any effects due to the change in band structure.

If the laser beam is focussed to a smaller spot the same number of excitons will be generated, but in a smaller volume. If an optical fibre is used to transmit the laser light to the sample this effect can be used to increase the concentration. The laser could be focussed with a strong lens outside the cryostat to a much smaller spot than could be obtained with the low power lens already in use, since the minimum spot size of a laser beam depends on the angle of the cone of the focussed ra-

Figure 4-1

Exciton spectrum under high stress. Note the shifting of the exciton peaks and "convex" rather than "concave" continuum region compared to the non-stressed case (see diagram 3-1).

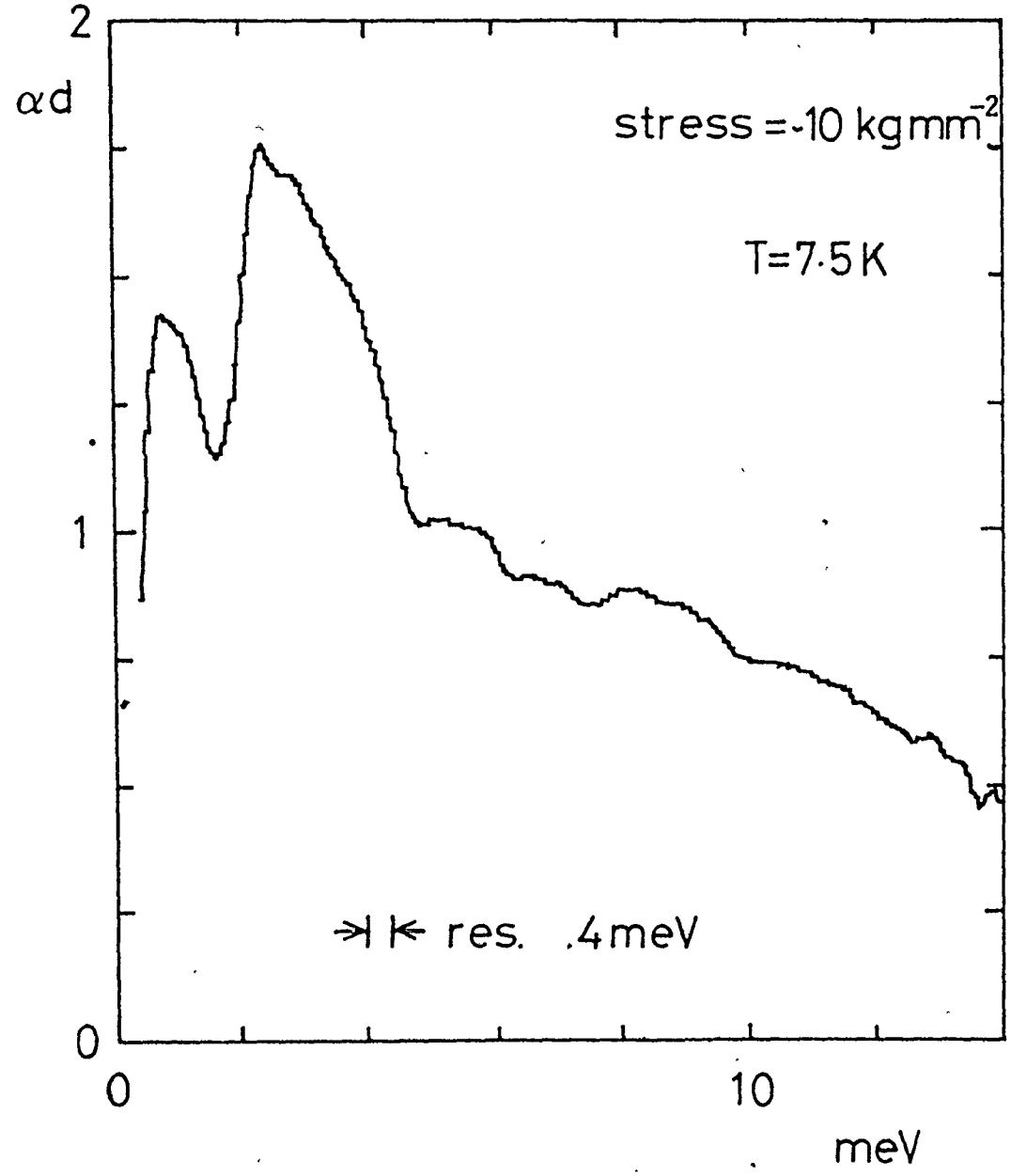
2
αd
stress =-10 kg mm⁻²
T=7·5 K
1
⇥I⇤ res. .4meV
0
0
10
meV

diation. The radiation would then be conducted to the surface of the crystal by the fibre, making sure that the beam divergence was within the acceptance angle for the fibre, so that total internal reflection would be obtained within the fibre and no light would be lost. The size of the spot on the sample could be varied by moving the fibre with respect to the sample or changing the position of the input beam at the fibre.

A single index, 0.2 mm diameter, teflon coated quartz fibre (of loss 3 dB/km) was installed in the equipment. The laser was focussed and introduced by means of a good quality microscope objective. At low temperatures however, no power could be detected at the sample. In a subsequent experiment a helium neon laser was focussed directly on the sample, and reflected light was observed at the input end of the fibre. In this way any misalignment with temperature change would not be seen. As the equipment cooled this reflected light gradually faded. The reason for this was later discovered by other workers (Katsuyama, et al. 1980) to be that as the fibre cools, the plastic sheath contracts more than the quartz, causing a compressive strain in the fibre which leads to loss of the light through bending losses. A simple experiment later demonstrated that if He-Ne light was passed through the fibre, and part of the fibre was cooled in liquid nitrogen vapour, light could be seen escaping in the cool region, with a corresponding loss of emergent light at the end. This effect was totally reversible

on warming the fibre.

Work is presently under way to investigate the properties of an uncoated fibre of much larger dimension, 1/8". Preliminary tests show that no low temperature losses occur with this fibre.

The laser was currently being used at its full single mode power, but four times as much power would be available if the higher order modes were allowed to propagate by removing the single mode aperture in the beam path. The divergence and minimum spot size of the multimode beam are much larger than those of the single mode, therefore improved focussing arrangements were required. Careful measurements were made of the profile of the laser beam as a function of distance from the laser, by traversing the beam with a fine slit and measuring the power transmitted, and investigations into the properties of materials for lenses were carried out. The lens had to be situated at the top of the far-infrared cone, within the cryostat, in order to maximize the focussing angle thereby minimizing the spot size, i.e. the lens had to be as close to the sample as possible.

Commercial infrared materials are available, but their properties have not been determined into the far infrared, and care had to be taken not to use a lens which, while focussing the laser, would block the far infrared radiation travelling the same path. Two main possibilities were considered: a lens made of glass (which blocks far-infrared radiation) of sufficiently small diameter to permit adequate far-infrared radiation

to pass, yet large enough to intercept most of the laser beam, and a lens made of TPX (a thermoplastic) which passes far-infrared. The refractive index of TPX was measured and found to be 1.51±0.03 for red light, and the specifications for a suitable lens were determined.

The TPX lens was abandoned due to the difficulties of manufacturing this very soft material into a high quality lens of good surface finish. It would also be very delicate in use. Instead a glass lens of 6 mm diameter and 20 cm focal length, and a holder, designed to block a minimal amount of radiation, were obtained. This enabled the multimode beam to be focussed to a spot of diameter 1.1 mm. Measurements showed that a maximum of three times the power could be obtained at the sample, approximately 25% of the multimode beam power being lost due to the extra lens and holder. This, if obtained, would produce a greater absorption of light than could usefully be measured ($\alpha d = 6$, see chapter 2), and thus represents the limit of this experimental system. No further increase of concentration could even be observed by the absorption of far-infrared radiation.

The main problem with obtaining this absorption of power was that the alignment of the system had become much more crucial. The finer, single-mode beam would pass through the aperture at the top of the light pipe with little danger of touching the side of the aperture and could just be pointed at the aperture at the sample. The multimode beam had to pass exactly

through the centre of the aperture since it was of the same diameter, through the centre of the small lens, and meet exactly the sample aperture. The easiest way to achieve this was to move the aperture at the sample to approximately the correct position and make a fine adjustment by moving the lens, which was achieved by bending the light pipe slightly. The cam and wedge system was used for this, see diagram.

The alignment could be checked visually by seeing the reflective surface of the sample when looking down the light pipe, and electrically by measuring the resistance of the sample when the laser impinged on it. The visual method was used to check the alignment before the experiment, and also during the cooling, as misalignment could sometimes occur at this stage.

In the resistance method, the thermocouple was used as one contact and the cryostat as the other. As the sample cooled, the resistance increased from kΩ to MΩ at 4.2°K, and, when the laser was aligned, decreased to the order of ohms if very good alignment was achieved. Thermal changes induced in the sample by the laser could be seen as a very slow drift in resistance. Photoexcitation of carriers was seen as an abrupt effect. This method is more useful than the normal procedure of checking the absorption of far-infrared radiation at the central maximum of the interferogram. It can be used before the detector has been cooled to liquid ^{3}He temperature. It will detect the onset of alignment at a much lower concentration of carriers, and is in-

Figure 4-2

The lightpipe bending apparatus. The block is fixed firmly to the lightpipe (part (i)) and the pipe is bent in two orthogonal directions by rotating the cam, and pulling up the conical wedge, which then push against the block, being held in place by the centering plate. The lightpipe is free to move inside the centering plate. View (ii) shows the lens and lens holder.

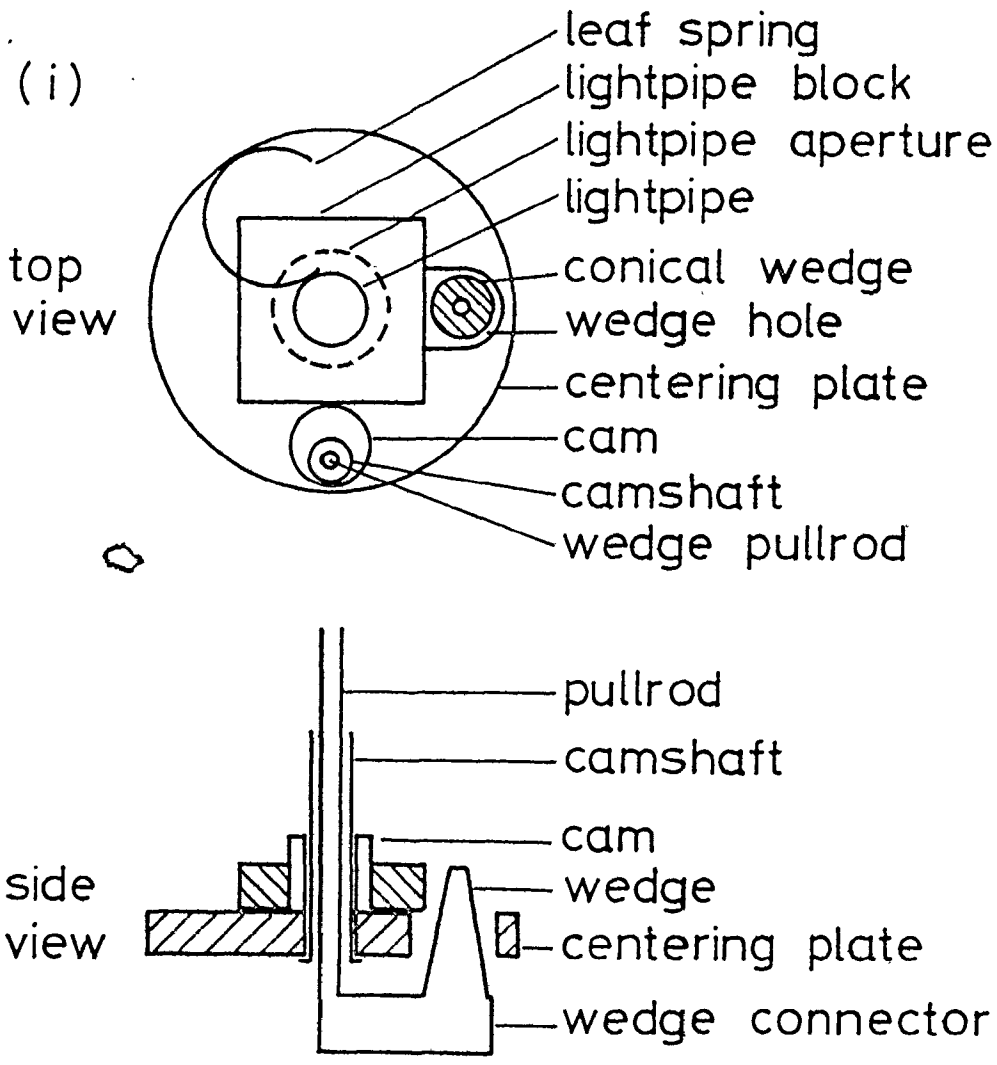
(i)
top view
leaf spring
lightpipe block
lightpipe aperture
lightpipe
conical wedge
wedge hole
centering plate
cam
camshaft
wedge pullrod
side view
pullrod
camshaft
cam
wedge
centering plate
wedge connector

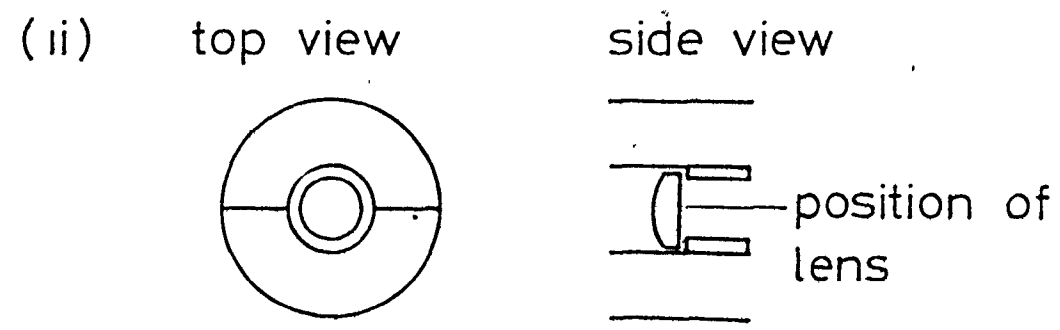
(ii)
top view
side view
position of lens

sensitive to the spectral range of the far infrared filters, which can cause the laser to be seen as misaligned if the region under observation contains no exciton or fluid absorption peaks.

Of the experiments performed using these techniques, three were productive: the results of these will be described in the next section.

(iii) Results

Of the three experiments mentioned in section (ii) the first gave the highest concentration of excitons. It was of limited success since a small capacity helium dewar was used (for later experiments a larger one was obtained) which means that the temperature stability was poor and the running time was short, since the high laser power evaporates the helium quickly. The results suggested, however at very high concentrations a new, previously unobserved, broad, peaked absorption of far-infrared radiation occurred between 1 and 2 meV*. This absorption was comparatively small ($\alpha d = 1.5$) at 4.2°K but nearly saturated at 7°K ($\alpha d = 3.5$). For both spectra all other absorption (from approximately 2 meV to 4 meV) was saturated (i.e. so close to 100% absorption that only noise could be seen: $\alpha d = 4$ or above).

---

*Buchanan and Timusk (1976) observed a peak from 1.2 - 1.5 meV which was much sharper than this one, and seen at lower concentrations.

This result was confirmed by the next experiment, where concentrations of approximately 50% of those of the first were obtained. The concentration could not be estimated from the height of the 3 meV peak in the normal way due to the saturation effect, but a low power spectrum was taken for comparison with ordinary exciton spectra, and in this one the peak could be seen. A rough estimate of the higher power spectra could then be obtained if the assumption was made that exciton concentration increased linearly with laser power, as it would be expected to do at the temperatures of these experiments (Timusk 1976). The maximum estimated concentration obtained in the first experiment was 3×10^{15} cm^{-3} and in the second $\sim$ 1.6 10^{15} cm^{-3}. The Mott criterion is 1.6×10^{15} cm^{-3}. If the concentration estimates are correct the data should contain information relevant to the metal-insulator transition.

As in the previous experiment the broad absorption seen between 1 and 2 meV was the most obvious feature of the data. It was present at 4.2°K as a shoulder on the 2.5 meV peak of normal exciton spectra. At 5°K it had developed into a very broad (full width at half maximum height of the order of 1 meV) smooth peak, centering at about 1.5 (± .15) meV. The third experiment suggested that any apparent structure on this peak was probably due to noise since it became smoother as more data were averaged in, although the possibility of structure could not be ruled out entirely. As the temperature was increased from 5°K to 7.5°K little change was seen in the height of this peak, but

Figure 4-3

Experimental data: 1.5 meV peak. Data (from run E15) showing the 1.5 meV peak for a range of pumping powers and temperatures.

Axes :-
vertical αd
horizontal meV

Concentration :-
(cm^{-3})

a 2×10^{14}
b 4×10^{14}
c 8×10^{14}
d 1.6×10^{15}

Resolution :-
0.06 meV

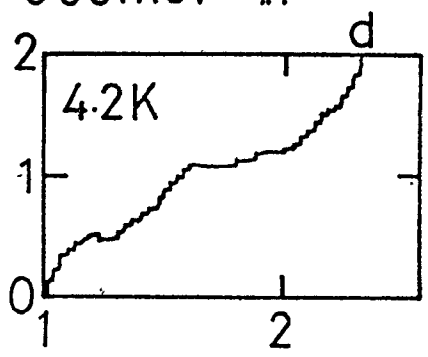

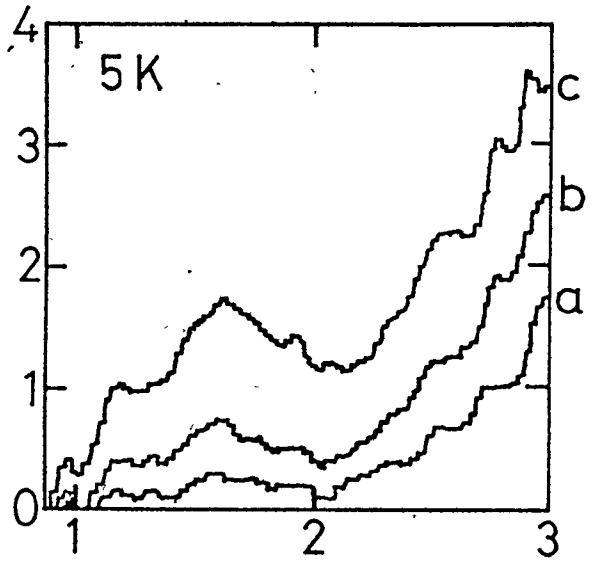

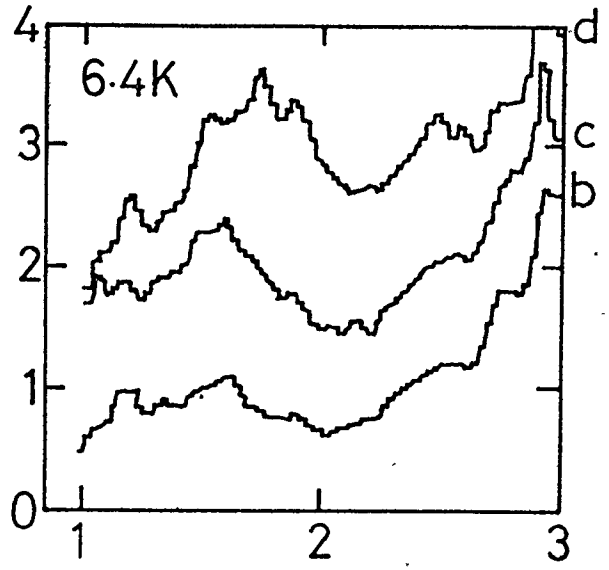

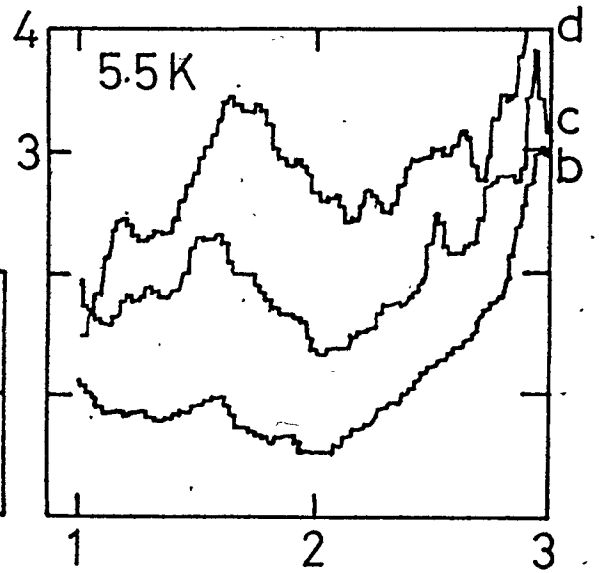

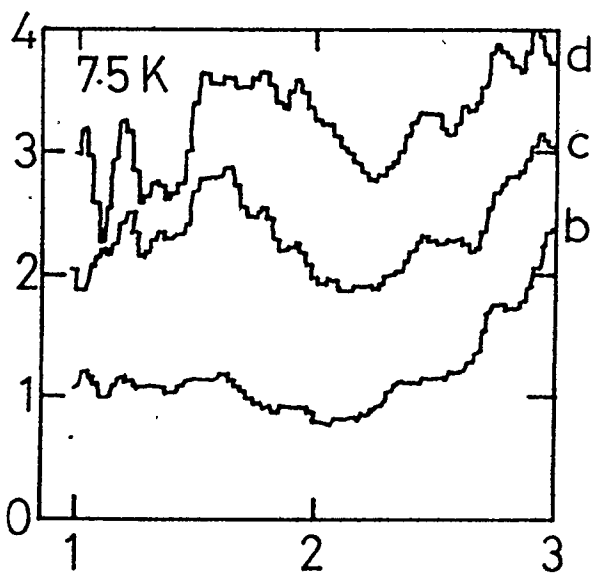

the height clearly depended on the pumping power. In the low power comparison spectrum corresponding to a concentration of 2×10^{14} cm^{-3} the peak was just starting to appear. The height of the peak appeared to increase approximately as the 1.5 power of that of the exciton peak at 2.5 meV, or of the pumping power.

No clear evidence was seen of a constant plasma absorption below 2 meV as observed by Timusk (1976): possibly this was there but was small compared to the main absorption and therefore could not be separately identified, or perhaps this absorption was a lower power precursor of the present data. If there is a constant background underlying the 1.5 meV peak it depends on concentration rather than temperature, at 5.5°K or above.

The low power exciton spectrum agrees well with the data of Timusk (1976) and Navarro (1979). The peaks do, however, appear to be less well resolved in the present data although the experimental resolution is nominally the same (0.05 meV). As the power increased the peaks became even broader until the peak at 2.5 meV could no longer be seen separately from the 3 meV peak. The 3 meV peak coincided with the onset of the saturated region in the higher power spectra (8×10^{14} cm^{-3} and 1.6×10^{15} cm^{3}) but a region of lower absorption could be seen after this peak in the 4×10^{14} cm^{-3} spectrum. For concentrations of 4×10^{14} cm^{-3} and above the absorption in this region appeared to be almost flat, and higher, in proportion to the 3 meV peak, than in the case of lower concentrations. In the spectrum at 2×10^{14} cm^{-3}

Figure 4-4

A spectrum compared to those of other workers

HN : Navarro (1979)

TT : Timusk (1976)

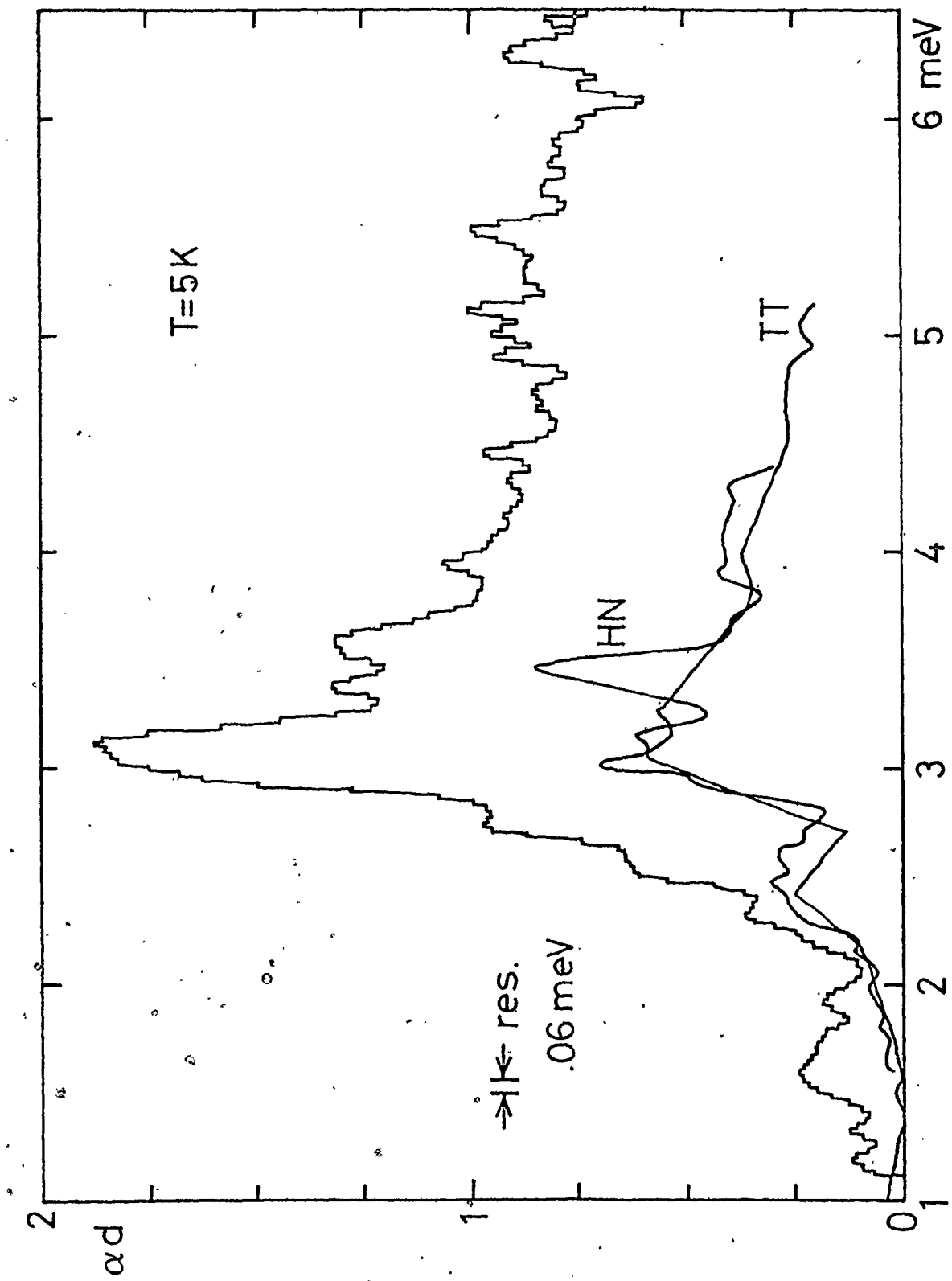
αd
2
1
0
1
2
3
4
5
6 meV
T=5K
HN
TT
res.
.06 meV

the absorption in this region (which corresponds to transitions to the ionization continuum) showed a $\nu^{-0.7}$ dependence. This could be accounted for by a constant, or nearly so, background absorption that depended on concentration. The data below 1 meV are noisy, but do seem to suggest that for spectra at 5.5°K and above the absorption at the low energy tail of the 1.5 meV peak does not go to zero but remains finite, and probably increases with concentration.

Finally another very low intensity, broad, peak centering between 5 and 6 meV was seen on all the data of concentration 2×10^{14} cm^{-3} up to 8×10^{14} cm^{-3}. Some spectra at the latter concentration and all at higher concentrations came too noisy for this peak to be determined. The height of the additional absorption was only of the order of 10% of the continuum absorption.

To summarize then, the most obvious feature of these data was the broad absorption at 1.5 meV. Besides this, broadening of the exciton peaks and possibly a flat, or very slowly varying background absorption with a broad peak at 5 - 6 meV were seen. All of these were concentration dependent. The only temperature dependence occurred fairly rapidly between 4.2°K and 5.5°K when the 1.5 meV peak appeared as a small shoulder and rapidly developed. The slowly varying background was present above 5.5°K. No abrupt change as a function of concentration was observed.

Figure 4-5

A complete energy range spectrum. The peak at 1.5 meV, the exciton peaks (2 - 4 meV) and the weak sbsorption peak at 5 - 6 meV can be seen.

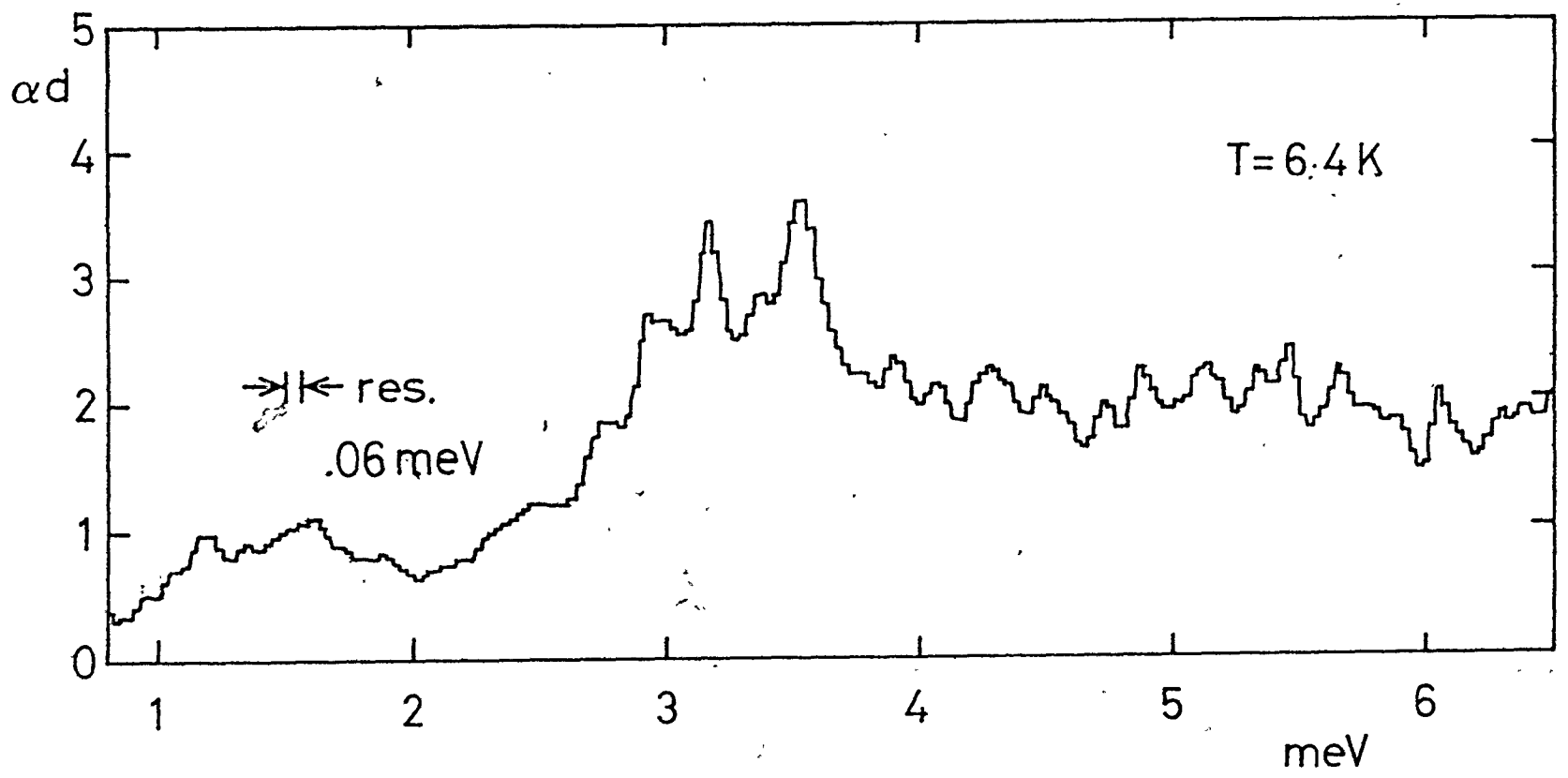
αd
5
4
3
2
1
0
T= 6.4 K
res.
.06 meV
1
2
3
4
5
6
meV

(iv) Discussion

The concentrations for these experiments were determined spectroscopically, in the manner detailed in chapter three, for lower concentrations ($\alpha d = 2$) and scaled to higher concentrations assuming that the laser power is used equally efficiently at all concentrations. An estimate was made of the effect collision broadening would have on the linewidth of the spectra to see if the concentration estimates could be confirmed and the observed broadening explained.

Assuming that the excitons each occupy a volume equivalent to the reciprocal of the concentration (n) and that the distance an exciton travels before colliding with another corresponds to a sphere of this volume a collision length (λ) can be obtained:

$$\frac{1}{n} = \frac{4}{3}\cdot\pi\lambda^3.$$

If the exciton travels at a thermal velocity given by $\frac{1}{2}mv^2 = kT$ the time between collisions (τ) can be determined. (It is possible to neglect the natural lifetime of the excitons in this estimate since the collision lifetime is a factor of 10^6 shorter.) This is related to the half width at half maximum height, Γ, of a Lorentzian shaped peak by $\tau = \frac{\hbar}{2\Gamma}$ where the amplitude of the peak is given by $A \propto \frac{\Gamma}{(\omega-\omega_0)^2+\Gamma^2}$. At $n = 2\times10^{14}$ cm^{-3} this corresponded to $\Gamma = 0.05$ meV. Unfortunately, Γ cannot be clearly measured from our data since it is of the order of the sepa-

ration between the lines due to the transitions between the split 1s and 2p states. The broadening did appear to be greater than 0.05 meV, however, and increased with concentration. In the limit that the broadening becomes much larger than the separation between the lines a Lorentzian lineshape could again be applied, but this limit was not reached.

Another possibility is that the concentration of excitons in the sample is non-uniform, and that regions of very high concentration occur where the laser strikes the sample. This would explain the fact that the spectra in these experiments, with the laser used multimode, appear broader than those where the laser is used single-mode, for similar concentrations, since the power/unit area at the surface of the crystal is 2 - 4 times higher in the former case. It is almost certain that parts of the exciton cloud were at a density greater than the metal-insulator transition density, which we take to be 1.6×10^{15} cm^{-3}, particularly for higher density spectra. The broadening is not due to a local high temperature in the crystal since no thermal plasma absorption was seen.

When the metal-insulator transition is observed for donors in semiconductors, firstly, as the concentration increases the electronic transition lines for individual donors come broadened, on the lower energy edge, which is often more readily observed, and then become completely merged so that a smooth broad absorption that occupies the same spectral

region as these lines, i.e. not extending to zero energy, is seen (see e.g. Capizzi et al. 1979). This is approximately what is seen in our data. At the two extremes of the non-uniform concentration model just discussed, the strongly absorbing higher concentration would give a smooth absorption and the lower concentration region would give small exciton peaks, and the two would be superimposed. A non-uniform exciton concentration would preclude the observation of abrupt changes at the onset of the transition as concentration was varied, whether or not these occurred.

In contrast to the concentration dependence the temperature effects on the spectra are noticed within a relatively small range of temperature. This seems to suggest the crossing of a phase boundary as temperature is increased. This temperature range overlaps the undetermined region in the phase diagram (see chapter two). Here the work of Thomas et al. (1973) on the liquid boundary, which is extrapolated past the critical point by fitting it to a universal liquid gas phase diagram (after Guggenheim, 1945) does not smoothly meet the gas liquid coexistence line (as was first pointed out by Timusk, 1976) obtained by threshold measurements of the appearance of electron-hole drops in the exciton spectrum, as obtained by Pokrovskii (1972), Hensel et.al. (1973), McGroddy et al. (1973), Lo et al. (1973), Benoît à la Guillaume et al. (1974), Westervelt et al. (1974) and Timusk (1976). In fact there is an absence of experimental data between $n_{ex} \sim 2\times10^{14}$ cm^{-3} and $\sim 8\times10^{16}$ cm^{-3}. The concentrations measured cover at least part of this region.

The broad absorption at 1.5 meV is, in shape, reminiscent of the electron-hole fluid absorption at 9 meV, and could perhaps be due to droplets of a similar electron-hole fluid, occurring at higher temperatures, such as the plasma that would be found when the metal-insulator transition took place. A possible modification of the phase diagram is shown. Phase diagrams of this form are obtained theoretically by Kraeft et al. (1975) and Sander and Fairobent (1976).

As the temperature is increased the dashed line (AC) is crossed and metallic plasma is formed in drops. This corresponds to the observed onset between 4 and 5.5°K of the peak as determined from plots of peak height against temperature for different pumping powers. As the pumping power is increased the size of, and volume occupied by, the plasma drops increases relative to the concentration of excitons until only plasma drops exist and no excitons are left, in an analogous way to ordinary electron-hole fluid.

The heavy solid lines represent behaviour determined experimentally. The lower concentration line, i.e. the exciton/electron-hole plasma coexistence line (AB), does not move above a concentration of 4×10^{14} cm^{-3} up to 7.5°K, since at no time was the concentration of plasma drops observed to go to zero as the temperature was increased, for this concentration.

The onset of the plasma drops occurs at 2×10^{14} cm^{-3}. The position of the higher concentration line (CD) was deter-

Figure 4-6

Modified phase diagram showing electron-hole plasma/exciton coexistence region. The thin solid lines are due to previous workers. The thick solid and dashed lines, AB, CD and AC are the result of the work described herein. The thin dashed lines are hypothetical.

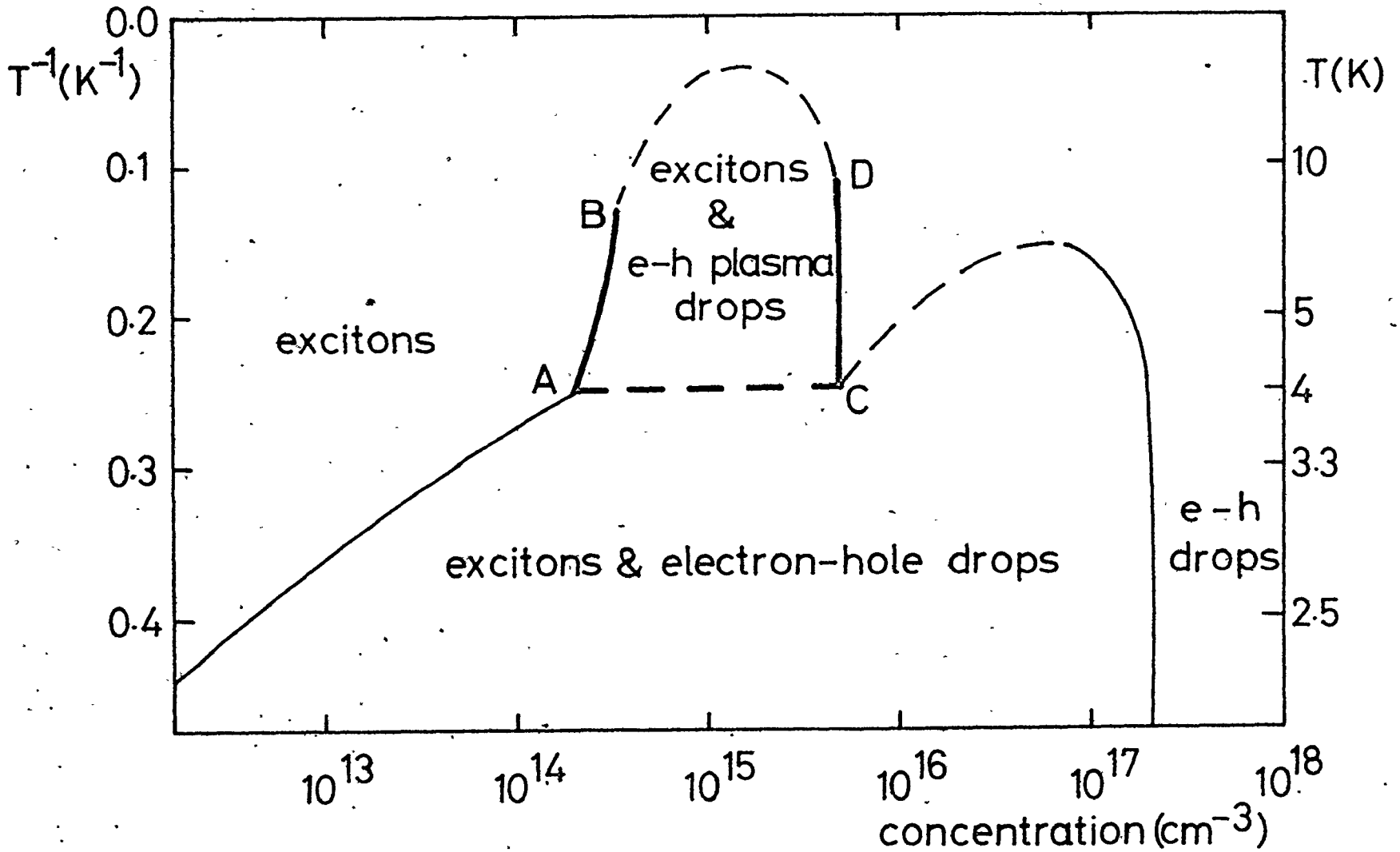
0·0
T⁻¹(K⁻¹)
0·1
0·2
0·3
0·4
T(K)
10
5
4
3·3
2·5
excitons
B
excitons
&
e-h plasma
drops
D
A
C
excitons & electron-hole drops
e-h
drops
10¹³
10¹⁴
10¹⁵
10¹⁶
10¹⁷
10¹⁸
concentration (cm⁻³)

mined by comparison with electron-hole drops. The concentration of pairs within a drop is given by $\omega_p^2 = ne^2/m$ where ω_p is the plasma frequency, e and m the charge and mass of the particles, and n the concentration. We take the ratio of the concentrations of electron-hole pairs in the ordinary electron-hole fluid and in plasma drops to be equal to the ratio of the squares of their observed resonant frequencies. This gives a value for the density of pairs in plasma drops of 5×10^{15} cm^{-3} (assuming $n_{drops} = 2\times10^{17}$ cm^{-3}, and that the peak is observed at 9 meV, see e.g. the thesis of G. Zàrate, 1981). Since the peak does not shift as the temperature changes, within the range measured, the line on the phase diagram must be very nearly vertical. An increase in the concentration results in the size of the drops increasing, rather than a change in the concentration of the pairs, which is characteristic of a condensed phase.

An alternative possibility for the 1.5 meV absorption is the formation of pairs of excitons into biexcitons, the equivalent of the hydrogen molecule. Thomas and Rice (Thomas et al. 1977) performed a luminescence experiment in germanium in which they saw a broadening on the exciton line. By calculating the shape of the exciton spectrum and the biexciton spectrum and adding them to fit their data they concluded that the broadening was due to the presence of biexcitons. They studied

this component at temperatures of 5.5°K and higher, and found that it had a 1.5 power dependence on exciton concentration, comparable to the value for our 1.6 meV peak, this being the only comparison which could be made. Balslev and Furneaux (Balsev and Furneaux 1979) attribute a similar observation to a metallic plasma produced by the metal insulator transition, however, and suggest an amendment to the phase diagram, similar to that already discussed. Miniscalco et al. (1977) also observe a component in their luminescence experiments in germanium which they attribute to a plasma, likewise Shah et al. (1977) for silicon. On balance, most evidence seems to favour the formation of a plasma.

Broadening of the lines in the donor problem is attributed to the formation of pairs of donors (e.g. Toyotomi 1975; Townsend 1978), but this situation is not really comparable to ours since the separation of the pairs varies from pair to pair and is fixed: they do not become bound at an equilibrium distance like biexcitons.

CHAPTER 5

SUMMARY AND DISCUSSION

In the work on the photo-ionization of excitons in germanium (chapter three) it was discovered that the frequency dependence of the cross-section varies as the - 1.4 (±0.2) power of the absorbed frequency for isolated excitons, rather than the - 2.67 predicted by hydrogenic theory. A theory specific to the case of excitons in germanium is not available. This phenomenon was compared to the case of donor impurities in germanium: here a similar - 1.5 frequency dependence occurs although hydrogenic behaviour is expected. In the donor problem this is explained by screening of the potential between the electron and the donor ion (the Lucovsky model). A justification of the application of this model to excitons was given, since the strength of the potential between the electron and the hole depends on the dielectric constant of germanium, which changes as the electron and hole approach one another closely. An examination of the effects of this correction, which is always neglected in exciton theory, on the theory is required, in order to see if the anomalous frequency dependence of the ionization can be explained, and check that the agreement between the theoretically and experimentally determined energy level schemes would not be seriously disturbed.

Experimentally, the effects of stress on the continuum could be investigated. A uniform stress applied to germanium in the <111> direction removes many of the degeneracies in the band structure: the conduction band minima are shifted, with the one in the stress direction being lowered in energy and the other three raised, so that only the lowest is populated, and the valence band maximum is split into two branches. At very high stresses the warping of the valence band constant energy surfaces is removed and they become ellipsoids. The band structure is thus very much simplified. One experiment of this kind was performed (chapter four), but rather than approaching the hydrogen result, the spectrum appeared to be totally different. This may be due to the photo-ionization or the appearance of a new absorption.

As concentration is increased the frequency dependence becomes weaker. A satisfactory explanation for this, in terms of present knowledge, was not found. The presence of a background absorption that varies with concentration, but only weakly with frequency, was proposed. The higher concentration work (chapter four) showed that the continuum absorption became even flatter as the concentration increased, but a flat background absorption could not be isolated in the spectrum since absorption peaks were seen in all regions investigated (excitons at 2 - 4 meV; a broad peak at 1 - 2 meV, peaking at 1.5 meV; and a barely present broad absorption at 5 - 6 meV, on top of the

continuum absorption). If more investigations were performed at extended energy ranges it would be possible to check whether the 5 - 6 meV absorption had a large enough range to affect the apparent frequency dependence of the ionization continuum. This absorption was not seen in the earlier, wider range, experiments due to the lower concentrations obtained. An experiment of this type could also be used to check the behaviour of the proposed electron-hole plasma drops. If the range covered included the ordinary electron-hole fluid peak position (9 meV) and the concentration was high enough to see the 1.5 meV peak, the temperature could be lowered so that the boundary AC (see phase diagram, chapter four) would be crossed. It should be observed that the 1.5 meV peak disappears and the 9 meV peak appears in its place.

Other experimental checks on the proposed phase diagram could include onset measurements of the 1.5 meV peak. The height of the peak would be measured as a function of temperature for a range of different concentrations between 2 and 4×10^{14} cm^{-3}, and the point at which it disappeared established. This would more accurately place the line AB. If a much thinner sample could be prepared the line AB could be extended to higher concentration. At present, the absorption, αd, reaches nearly 100% for much of the range of power obtainable from the laser. If the thickness of the crystal was reduced below the exciton cloud diffusion radius ($\sim$ 1 mm) higher values of α could be observed before saturation of the spectrum occurred. The concentration

would possibly be increased since the excitons would be more confined. Experimental difficulties would include the need for a very good surface on both sides of the crystal to avoid higher surface recombination, which would lower the concentration, and fragility of the crystal, since the area would have to remain large in order to dissipate the heat generated by the laser.

It has been shown that the absorption of far-infrared radiation by excitons in germanium reveals that new and interesting phenomena occur when the exciton concentration is increased above the limit where they may be considered to be isolated. This technique is more sensitive than the recombination luminescense technique and should be used to continue the work of resolving the uncertainty regarding the metal-insulator transition in excitons in germanium.

BIBLIOGRAPHY

M. Altarelli and N.O. Lipari, Proceedings of the 13th International Conference on the Physics of Semiconductors, Rome 1976, p. 811, ed. F.G. Fumi.

I. Balslev and J.E. Furneaux, Sol. St. Comm. 32, 609 (1979).

R.J. Bell, "Introductory Fourier Transform Spectroscopy", Academic Press (1972).

C. Benoît à la Guillaume, M. Capizzi, B. Etienne, and M. Voos, Sol. St. Comm. 15, 1031 (1974).

H.A. Bethe and E.E. Salpeter, "Quantum Mechanics of One- and Two-electron Atoms", Springer Verlag, 1957.

W.F. Brinkman and T.M. Rice, Phys. Rev. B 7, 1508 (1973).

M. Buchanan and T. Timusk, Proc. 13th International Conference on the Physics of Semiconductors, Rome, 1976, p. 821, Ed. F.G. Fumi.

M. Capizzi, G.A. Thomas, F. DeRosa, R.N. Bhatt and T.M. Rice, Sol. St. Comm. 31, 611 (1979).

D.D. Clayton, "Principles of Stellar Evolution and Nucleosynthesis", McGraw Hill (1968).

G. Dresselhaus, J. Phys. Chem. Solids 1, 14 (1956).

E.A. Guggenheim, J. Chem. Phys. 13, 253 (1945).

H. Haken, "Quantum Field Theory of Solids, an Introduction", North-Holland Publishing Co., 1976.

E.E. Haller and W.L. Hansen, IEEE Trans. Nucl. Sci. 21, 279 (1974).

J.C. Hensel, T.G. Phillips and T.M. Rice, Phys. Rev. Lett. 30, 227 (1973).

H. Hertz, J. Math. (Crelle's J.) 92, 156 (1881).

E.O. Kane, Phys. Rev. B 11, 3850 (1975).

Y. Katsuyama, Y. Mitsunaga, Y. Ishida and K. Ishihara, Appl. Opt. 19, 4200 (1980).

C. Kittel, "Introduction to Solid State Physics", 5th Ed., John Wiley and Sons Inc. (1976).

W.D. Kraeft, K. Killiman and D.Kremp, Phys. Stat. Sol. (b) 72, 461 (1975).

L. Landau and G. Zeldovich, Acta Phys.-Chim. USSR 18, 194 (1943) Translated in "Collected Papers of Landau", Ed. D. ter Haar, Gordon and Breach (1965).

T.K. Lo, B.J. Feldman and C.D. Jeffies, Phys. Rev. Lett. 31, 224 (1973).

G. Lucovsky, Sol. St. Comm. 3, 299 (1965).

O. Madelung, "Introduction to Solid-State Theory", Springer Series in Solid-State Sciences, Vol. 2, Springer-Verlag (1978).

R.S. Markiewicz, J.P. Wolfe and C.D. Jeffries, Phys. Rev. B 15, 1988 (1977).

J.C. McGroddy, M. Voos and O. Christensen, Sol. St. Comm. 13, 1801 (1973).

W. Miniscalco, C.-C. Huang and M.B. Salamon, Phys. Rev. Lett. 39, 1356 (1977).

K.D. Möller and W.G. Rothschild, "Far-Infrared Spectroscopy", Wiley-Interscience (1971).

N.F. Mott, "Metal-Insulator Transitions", Taylor and Francis Ltd. (1974).

H. Navarro, Ph.D. Thesis, McMaster University (1979).

Ya. E. Pokrovskii, Phys. Status Solidi A 11, 385 (1972).

Ya. E. Pokrovskii and K.I. Svistunova, Fiz. Tverd. Tela. 13, 1485 (1971), (Sov. Phys. Solid State 13, 1241 (1971)).

T.M. Rice, Proc. 12th Int. Conf. Phys. Semiconductors, Stuttgart (1974), p. 23, Ed. M.H. Pilkuhn.

L.M. Sander and D.K. Fairobent, Sol. St. Comm. 20, 631 (1976).

J. Shah, M. Combescot and A.H. Dayem, Phys. Rev. Lett. 38, 1497 (1977).

M. Shinada and S. Sugano, J. Phys. Soc. Japan 21, 1936 (1966).

G.A. Thomas, T.G. Phillips, T.M. Rice and J.C. Hensel, Phys. Rev. Lett. 31, 386 (1973).

G.A. Thomas and T.M. Rice, Sol. St. Comm. 23, 359 (1977).

T. Timusk, Phys. Rev. B 13, 3511 (1976).

T. Timusk and K.F. Lin, Proc. 35th Symp. on Molecular Spectroscopy, Columbus,Ohio, page 68 (1980).

P.J. Townsend, J.Phys. C.: Sol. St. Phys. 11, 1481 (1978).

S. Toyotomi, J. Phys. Soc. Jpn. 38, 175 (1975).

R.M. Westervelt, T.K. Lo, J.L. Staehli and C.D. Jeffries, Phys. Rev. Lett. 32, 1051 (1974); 32, 1331 E (1974).

G. Zárate, Ph.D. Thesis, McMaster University (1981).